Journal of Inequalities and Applications
a SpringerOpen Journal

RESEARCH Open Access

Dynamics analysis and optimal control of delayed SEIR model in COVID-19 epidemic

Chongyang Liu[1,2*], Jie Gao[3†] and Jeevan Kanesan[4†]

*Correspondence:
chongyangliu@aliyun.com
[1]School of Mathematics and Information Science, Shandong Technology and Business University, Yantai 264005, P.R. China
[2]Yantai Key Laboratory of Big Data Modeling and Intelligent Computing, Yantai, 264005, P.R. China
Full list of author information is available at the end of the article
[†]Equal contributors

Abstract

The coronavirus disease 2019 (COVID-19) remains serious around the world and causes huge deaths and economic losses. Understanding the transmission dynamics of diseases and providing effective control strategies play important roles in the prevention of epidemic diseases. In this paper, to investigate the effect of delays on the transmission of COVID-19, we propose a delayed SEIR model to describe COVID-19 virus transmission, where two delays indicating the incubation and recovery periods are introduced. For this system, we prove its solutions are nonnegative and ultimately bounded with the nonnegative initial conditions. Furthermore, we calculate the disease-free and endemic equilibrium points and analyze the asymptotical stability and the existence of Hopf bifurcations at these equilibrium points. Then, by taking the weighted sum of the opposite number of recovered individuals at the terminal time, the number of exposed and infected individuals during the time horizon, and the system cost of control measures as the cost function, we present a delay optimal control problem, where two controls represent the social contact and the pharmaceutical intervention. Necessary optimality conditions of this optimal control problem are exploited to characterize the optimal control strategies. Finally, numerical simulations are performed to verify the theoretical analysis of the stability and Hopf bifurcations at the equilibrium points and to illustrate the effectiveness of the obtained optimal strategies in controlling the COVID-19 epidemic.

Keywords: Delayed SEIR; Stability; Hopf bifurcation; Optimal control; Necessary optimality conditions; Numerical simulation

1 Introduction

The coronavirus disease 2019 (COVID-19) is an epidemic caused by the SARS-CoV-2 virus, which affects mostly the human respiratory system. Due to the strong infectivity, fast transmission speed, and long incubation period, it has brought significant losses to human life and the global economy [1, 2]. Although many prevention and control measures have been taken to mitigate the disease spread, the world is still suffering from the infection and death cases of COVID-19. According to the World Health Organization report, as of 2 November 2023, the total number of infections caused by the COVID-19 epidemic has reached 697,318,367, with more than 6,934,066 deaths [3]. Thus, there is an urgent need to

study the COVID-19 virus transmission behavior and provide effective control measures to prevent the spread of the disease.

Mathematical models have been proven effective means in describing and understanding the complex transmission dynamics of epidemics [4–6]. In this regard, several mathematical models have been investigated to formulate and control COVID-19 spread [7–9]. SIR (Susceptible, Infectious, Removed) models have been proposed to simulate and predict the COVID-19 pandemic in [10, 11]. The stability of the SEIR (Susceptible, Exposed, Infectious, Removed) model is analyzed in [12]. Stability analysis of a spatial extension of the SEIR model is carried out in [13]. Optimal control of both non-pharmacological and pharmacological interventions for a modified SEIR epidemiological model is studied in [14]. Optimal control of COVID-19 spread considering quarantine effect on people with diabetes is investigated in [15]. Stability analysis and optimal control of a COVID-19 system, including susceptible, exposed, symptomatically infected, asymptomatically infected, hospitalized, and recovered individuals, are discussed in [16]. Bifurcation analysis and optimal control of a discrete SIR system are studied in [17]. Optimal control of the Omicron and Delta strains in COVID-19 is investigated in [18]. Although the aforementioned results are certainly valid and interesting, time delays are ignored in the dynamics analysis and optimal control problems. In fact, time delays exist in COVID-19 virus transmission since there is an incubation period for the exposed individual to manifest COVID-19 symptoms and signs, and a recovery period is required for the infected individual to become a recovered individual [19, 20].

Motivated by the above issue, in the current paper, we propose a delayed SEIR model to describe COVID-19 virus transmission in which two delays representing the incubation period and the recovery period are introduced. For this delayed SEIR system, we prove that its solutions with the nonnegative initial conditions are nonnegative and ultimately bounded. Furthermore, we calculate the disease-free and endemic equilibrium points and analyze the locally asymptotical stability and Hopf bifurcations of these two equilibrium points. Then, by taking the weighted sum of the opposite number of recovered individuals at the terminal time, the number of exposed and infected individuals during the time horizon, and the system cost of control measures as the cost function, we present a delay optimal control problem, where two controls denote the social contact and the pharmaceutical intervention. We also derive the necessary optimality conditions to characterize the optimal controls. Based on the necessary optimality conditions, we develop a numerical approach for solving the delay optimal control problem, which is different from the reported methods in [21–26]. Finally, numerical simulations are performed to verify the theoretical analysis of the stability and the existence of Hopf bifurcations at equilibrium points and demonstrate the effectiveness of computed optimal strategies in controlling the COVID-19 epidemic. Compared with the existing literature, the main contributions and innovations of this paper include: (i) a novel SEIR system with incubation and recovery delays is proposed for COVID-19 virus transmission; (ii) the stability and Hopf bifurcation of the equilibria in the delayed SEIR model are thoroughly analyzed; and (iii) an effective solution approach is developed for solving the delayed optimal control problem with both the terminal and integral costs.

The paper is organized as follows: In Sect. 2, the delayed SEIR system is proposed, and some important properties are proved. In Sect. 3, the stability and existence of Hopf bifurcations at the disease-free and endemic equilibrium points are analyzed. In Sect. 4, we

present the delay optimal control problem and derive the corresponding necessary optimality conditions. In Sect. 5, we illustrate the numerical simulation results. In Sect. 6, we provide conclusions.

2 Delayed SEIR model

In the COVID-19 virus transmission process, the primary source of transmission is social contact between susceptible and exposed individuals who are usually asymptomatic. Another transmission source is direct contact between frontline workers and infected individuals. Some exposed individuals usually recover due to their strong natural immune systems or use over-the-counter medications, while others require hospitalization after a certain incubation period. Many infected individuals recover from the disease after extensive treatment, but unfortunately, for some, the infection costs their lives. As is well-known, a susceptible individual does not show the corresponding symptoms quickly after infection with the virus; that is, there is an incubation period for the exposed individual to be an infective individual. Besides, it is required for the infected individual to spend some time to be a recovered individual. Thus, time delays must be incorporated into the COVID-19 virus transmission process. Based on SEIR system [14], we propose the following delayed SEIR system to describe the COVID-19 virus transmission:

$$\begin{cases} \dot{S}(t) = \Lambda - \frac{\beta_1 S(t)E(t)}{N(t)} - \frac{\beta_2 S(t)I(t)}{N(t)} - dS(t), \\ \dot{E}(t) = \frac{\beta_1 S(t)E(t)}{N(t)} + \frac{\beta_2 S(t)I(t)}{N(t)} - \varepsilon E(t-\tau_1) - (\gamma_2 + d)E(t), \\ \dot{I}(t) = \varepsilon E(t-\tau_1) - \gamma_1 I(t-\tau_2) - (\mu + d)I(t), \qquad t \geq 0, \\ \dot{R}(t) = \gamma_1 I(t-\tau_2) + \gamma_2 E(t) - dR(t), \end{cases} \tag{1}$$

where t is the time of process; $S(t)$, $E(t)$, $I(t)$, and $R(t)$ are, respectively, the susceptible, exposed, infected, and recovered individuals; $N(t) = S(t) + E(t) + I(t) + R(t)$ is the total number of individuals affected by the outbreak; Λ is the recruitment in the human population; d is the natural mortality rate; β_1 is the transmission rate due to social contact; β_2 is the transmission rate due to frontline contact; ε is the infection rate; γ_1 is the recovery rate of infectious individuals; γ_2 is the immune recovery rate; μ is the probability of death due to COVID-19; τ_1 and τ_2 are two delay arguments that indicate the incubation and recovery periods, respectively. A flow chart of the delayed SEIR system (1) is shown in Fig. 1.

For system (1), the initial conditions are given by

$$S(t) = \varphi_1(t), \qquad E(t) = \varphi_2(t), \qquad I(t) = \varphi_3(t), \qquad R(t) = \varphi_4(t), \tag{2}$$

where $t \in [-\tau, 0]$ with $\tau = \max\{\tau_1, \tau_2\}$; and φ_i, $i = 1, 2, 3, 4$, are given functions. For system (1) with the initial conditions (2), we have the following theorem:

Theorem 1 *If the initial conditions are as follows $\varphi_i \geq 0$, $i = 1, 2, 3, 4$, then the solutions of system (1) are nonnegative and ultimately bounded.*

Proof It is easy to show by Theorem 5.2.1 [27] that $S(t) \geq 0$, $E(t) \geq 0$, $I(t) \geq 0$ and $R(t) \geq 0$ for $t \geq 0$. Hence, the nonnegative cone $\mathbb{R}^4_+$ is invariant for system (1) with nonnegative

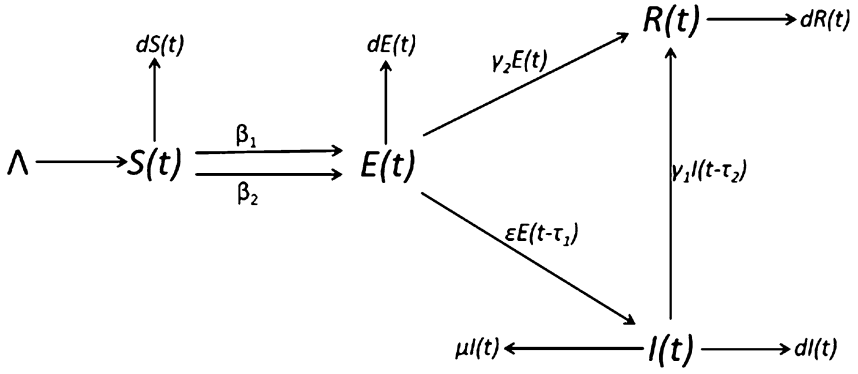

Figure 1 Flow chart of delayed SEIR model

initial conditions $\varphi_i \geq 0$, $i = 1, 2, 3, 4$. Furthermore, from (1), we have

$$\Lambda - (d + \mu)N(t) \leq \frac{dN(t)}{dt} = \Lambda - dN(t) - \mu I(t) \leq \Lambda - dN(t),$$

which gives

$$\frac{\Lambda}{d + \mu} \leq \liminf_{t\to\infty} N(t) \leq \limsup_{t\to\infty} N(t) \leq \frac{\Lambda}{d}.$$

Then, the delayed SEIR system (1) has a biologically feasible range as indicated below:

$$\left\{\big(S(t), E(t), I(t), R(t)\big) \in \mathbb{R}^4_+ : \frac{\Lambda}{d + \mu} \leq S(t) + E(t) + I(t) + R(t) \leq \frac{\Lambda}{d}, t \geq 0\right\},$$

which implies the ultimate boundedness of the solutions. □

3 Equilibrium points, stability and Hopf bifurcation

In this section, we will analyze the local stability of system (1) at the equilibrium points and establish the existence of Hopf bifurcations at the equilibrium points.

3.1 Equilibrium points

For system (1), the disease-free and the endemic equilibrium points are defined as

$$E_0 = \left(\frac{\Lambda}{d}, 0, 0, 0\right) \quad \text{and} \quad E_1 = \big(S^*, E^*, I^*, R^*\big), \tag{3}$$

where

$$\begin{cases} S^* = \frac{\Lambda(\varepsilon+\gamma_2+d)(\mu+\gamma_1+d)}{d[\beta_1(\mu+\gamma_1+d)+\varepsilon\beta_2]}, \\ E^* = \frac{-\Lambda(\varepsilon+\gamma_2+d)(\mu+\gamma_1+d)+\Lambda\beta_1(\mu+\gamma_1+d)+\Lambda\varepsilon\beta_2}{\varepsilon\beta_2(\varepsilon+\gamma_2+d)+\beta_1(\varepsilon+\gamma_2+d)(\mu+\gamma_1+d)}, \\ I^* = \frac{\varepsilon[\Lambda\beta_1(\mu+\gamma_1+d)+\Lambda\varepsilon\beta_2-\Lambda(\varepsilon+\gamma_2+d)(\mu+\gamma_1+d)]}{\beta_1(\mu+\gamma_1+d)^2(\varepsilon+\gamma_2+d)+\varepsilon\beta_2(\mu+\gamma_1+d)(\varepsilon+\gamma_2+d)}, \\ R^* = \frac{\gamma_1 I^*+\gamma_2 E^*}{d}. \end{cases} \tag{4}$$

Now, we consider the basic reproduction number R_0 [28], which can be used to determine whether a disease is an epidemic. To begin with, we rewrite system (1) as $\dot{x} = f - v$, where

$$x = \begin{pmatrix} S \\ E \\ I \\ R \end{pmatrix}, \qquad f = \begin{pmatrix} 0 \\ \frac{\beta_1 SE}{N} + \frac{\beta_2 SI}{N} \\ 0 \\ 0 \end{pmatrix}, \qquad v = \begin{pmatrix} -\Lambda + \frac{\beta_1 SE}{N} + \frac{\beta_2 SI}{N} + dS \\ \varepsilon E(t-\tau_1) + (\gamma_2 + d)E \\ -\varepsilon E(t-\tau_1) + \mu I + \gamma_1 I(t-\tau_2) + dI \\ -\gamma_1 I(t-\tau_2) - \gamma_2 E + dR \end{pmatrix}.$$

Then, by taking E and I as the infection compartments, we obtain the following Jacobian matrices F and V at the disease-free equilibrium point E_0:

$$F = \begin{pmatrix} \beta_1 & \beta_2 \\ 0 & 0 \end{pmatrix}, \qquad V = \begin{pmatrix} \varepsilon + \gamma_2 + d & 0 \\ -\varepsilon & \mu + \gamma_1 + d \end{pmatrix}.$$

Thus, R_0 can be defined as

$$R_0 = \rho\left(FV^{-1}\right) = \frac{\beta_1}{\varepsilon + \gamma_2 + d} + \frac{\beta_2 \varepsilon}{(\varepsilon + \gamma_2 + d)(\mu + \gamma_1 + d)}. \tag{5}$$

Furthermore, the endemic equilibrium point E_1 defined in (3) can be rewritten as

$$\left(\frac{\Lambda}{dR_0}, \frac{\Lambda}{\varepsilon + \gamma_2 + d}\left(1 - \frac{1}{R_0}\right), \frac{\Lambda\varepsilon}{(\mu + \gamma_1 + d)(\varepsilon + \gamma_2 + d)}\left(1 - \frac{1}{R_0}\right), \frac{\gamma_1 I^* + \gamma_2 E^*}{d}\right).$$

Therefore, system (1) has a positive endemic equilibrium point when $R_0 > 1$.

3.2 Stability and Hopf bifurcation of disease-free equilibrium point

The Jacobian matrix of system (1) at E_0 is given by

$$J_{E_0} = \begin{pmatrix} -d & -\beta_1 & -\beta_2 & 0 \\ 0 & -(\varepsilon e^{-\lambda\tau_1} + \gamma_2 + d) + \beta_1 & \beta_2 & 0 \\ 0 & \varepsilon e^{-\lambda\tau_1} & -(\mu + d + \gamma_1 e^{-\lambda\tau_2}) & 0 \\ 0 & \gamma_2 & \gamma_1 e^{-\lambda\tau_2} & -d \end{pmatrix}. \tag{6}$$

For (6), two negative eigenvalues are given by $\lambda_1 = \lambda_2 = -d$. The other two eigenvalues are determined by the following characteristic equation:

$$\lambda^2 + A_1^1\lambda + A_2^1 + \left(B_0^1\lambda + B_1^1\right)e^{-\lambda\tau_1} + \left(C_0^1\lambda + C_1^1\right)e^{-\lambda\tau_2} + D_0^1 e^{-\lambda(\tau_1+\tau_2)} = 0, \tag{7}$$

where $A_1^1 = \gamma_2 + d - \beta_1 + \mu + d$; $A_2^1 = (\gamma_2 + d - \beta_1)(\mu + d)$; $B_0^1 = \varepsilon$; $B_1^1 = \varepsilon(\mu + d - \beta_2)$; $C_0^1 = \gamma_1$; $C_1^1 = \gamma_1(\gamma_2 + d - \beta_1)$; and $D_0^1 = \varepsilon\gamma_1$.

Now, we study the following cases for delay arguments τ_1 and τ_2 at E_0.

Case 3.2.1 If $\tau_1 = \tau_2 = 0$, then equation (7) becomes

$$\lambda^2 + \left(A_1^1 + B_0^1 + C_0^1\right)\lambda + A_2^1 + B_1^1 + C_1^1 + D_0^1 = 0. \tag{8}$$

It follows from (5) that

$$R_0 = R_1 + R_2, \tag{9}$$

where $R_1 = \frac{\beta_1}{\varepsilon+\gamma_2+d}$; and $R_2 = \frac{\beta_2\varepsilon}{(\varepsilon+\gamma_2+d)(\mu+\gamma_1+d)}$. Obviously, $R_1 > 0$, and $R_2 > 0$. Let

$$\begin{cases} a_0^1 = 1, \\ a_1^1 = A_1^1 + B_0^1 + C_0^1 = \mu + \gamma_1 + \varepsilon + \gamma_2 + 2d - \beta_1 \\ \quad = (1 - R_1)(\varepsilon + \gamma_2 + d) + \mu + \gamma_1 + d, \\ a_2^1 = A_2^1 + B_1^1 + C_1^1 + D_0^1 = (\varepsilon + \gamma_2 + d - \beta_1)(\mu + \gamma_1 + d) - \beta_2\varepsilon \\ \quad = (1 - R_0)(\varepsilon + \gamma_2 + d)(\mu + \gamma_1 + d), \\ a_3^1 = 0. \end{cases}$$

Then, we have

$$a_1^1 a_2^1 > a_0^1 a_3^1, \quad \text{and} \quad a_i^1 > 0, \quad i = 0, 1, 2, \text{for } R_0 < 1,$$

and

$$a_2^1 < 0 \quad \text{for } R_0 > 1.$$

By the Routh-Hurwitz theorem [29], we obtain the following theorem:

Theorem 2 *Suppose that* $\tau_1 = \tau_2 = 0$.
(*i*) *If* $R_0 < 1$, *then* E_0 *is locally asymptotically stable*;
(*ii*) *If* $R_0 > 1$, *then* E_0 *is unstable*.

Case 3.2.2 If $\tau_1 = 0$, and $\tau_2 > 0$, then equation (7) turns to

$$\lambda^2 + \left(A_1^1 + B_0^1\right)\lambda + A_2^1 + B_1^1 + \left[C_0^1\lambda + \left(C_1^1 + D_0^1\right)\right]e^{-\lambda\tau_2} = 0. \tag{10}$$

Next, we will discuss the Hopf bifurcation of (10). Obviously, $\lambda = i\omega$ ($\omega > 0$) is a pure imaginary root of the equation (10) if and only if

$$-\omega^2 + \left(A_1^1 + B_0^1\right)i\omega + A_2^1 + B_1^1 + \left[C_0^1 i\omega + \left(C_1^1 + D_0^1\right)\right]\left[\cos(\omega\tau_2) - i\sin(\omega\tau_2)\right] = 0. \tag{11}$$

Separating the real part from the imaginary part in (11) gives

$$\begin{cases} \omega^2 - (A_2^1 + B_1^1) = C_0^1\omega\sin(\omega\tau_2) + (C_1^1 + D_0^1)\cos(\omega\tau_2), \\ -(A_1^1 + B_0^1)\omega = C_0^1\omega\cos(\omega\tau_2) - (C_1^1 + D_0^1)\sin(\omega\tau_2). \end{cases} \tag{12}$$

By adding the squares of two equations in (12), we obtain

$$\omega^4 + \left[\left(A_1^1 + B_0^1\right)^2 - 2\left(A_2^1 + B_1^1\right) - \left(C_0^1\right)^2\right]\omega^2 + \left(A_2^1 + B_1^1\right)^2 - \left(C_1^1 + D_0^1\right)^2 = 0. \tag{13}$$

Let $z = \omega^2$, $h_{01} = (A_2^1 + B_1^1)^2 - (C_1^1 + D_0^1)^2$ and $h_{11} = (A_1^1 + B_0^1)^2 - 2(A_2^1 + B_1^1) - (C_0^1)^2$. Then, equation (13) can be rewritten as

$$z^2 + h_{11}z + h_{01} = 0. \tag{14}$$

Without loss of generality, we assume that equation (14) has two positive roots, denoted by z_1 and z_2. Then, two positive roots of equation (13) are

$$\omega_2^1 = \sqrt{z_1} \quad \text{and} \quad \omega_2^2 = \sqrt{z_2}. \tag{15}$$

Furthermore, substituting (15) into (12) and solving the resulting equations, we have

$$\tau_2^{j,k} = \frac{1}{\omega_2^j}\left(\arccos\left[\frac{M_1M_3(\omega_2^j) + M_2M_4(\omega_2^j)}{M_1^2 + M_2^2}\right] + 2k\pi\right), \quad j = 1,2; k = 0,1,\ldots,$$

where $M_1 = C_1^1 + D_0^1$; $M_2 = C_0^1$; $M_3(\omega_2^j) = (\omega_2^j)^2 - (A_2^1 + B_1^1)$; and $M_4(\omega_2^j) = -(A_1^1 + B_0^1)\omega_2^j$. Clearly,

$$\lim_{k\to\infty} \tau_2^{j,k} = \infty, \quad j = 1,2.$$

Thus, we can define

$$\tau_2^0 = \min_{j\in\{1,2\}}\left\{\tau_2^{j,0}\right\}, \quad \text{and} \quad \omega_2^0 = \arg\min_{j\in\{1,2\}}\left\{\tau_2^{j,0}\right\}. \tag{16}$$

Now, we consider the roots of equation (10) as a function of τ_2 and the root $\lambda_1(\tau_2) = \xi_1(\tau_2) + i\omega_1(\tau_2)$ of equation (10) such that

$$\xi_1\left(\tau_2^0\right) = 0, \quad \text{and} \quad \omega_1\left(\tau_2^0\right) = \omega_2^0,$$

where τ_2^0 and ω_2^0 are as defined in (16). Substituting $\lambda_1(\tau_2)$ into equation (10) and taking the derivative with respect to τ_2, we have

$$\left(\frac{d\lambda_1}{d\tau_2}\right)^{-1} = \frac{2\lambda_1 + A_1^1 + B_0^1}{-\lambda_1[(\lambda_1)^2 + (A_1^1 + B_0^1)\lambda_1 + A_2^1 + B_1^1]} + \frac{C_0^1}{\lambda_1(C_0^1\lambda_1 + C_1^1 + D_0^1)} - \frac{\tau_2}{\lambda_1}.$$

Then,

$$\mathrm{Re}\left[\left(\left.\frac{d\lambda_1}{d\tau_2}\right|_{\tau_2=\tau_2^0}\right)^{-1}\right] = \frac{(M_1^1N_1^1 + S_1^1T_1^1)[(P_1^1)^2 + (O_1^1)^2] + (Q_1^1P_1^1)[(N_1^1)^2 + (T_1^1)^2]}{[(N_1^1)^2 + (T_1^1)^2][(P_1^1)^2 + (O_1^1)^2]},$$

where $M_1^1 = A_1^1 + B_0^1$; $S_1^1 = 2\omega_2^0$; $N_1^1 = (A_1^1 + B_0^1)(\omega_2^0)^2$; $T_1^1 = (\omega_2^0)^3 - (A_2^1 + B_1^1)\omega_2^0$; $Q_1^1 = C_0^1$; $P_1^1 = -C_0^1(\omega_2^0)^2$; and $O_1^1 = (C_1^1 + D_0^1)\omega_2^0$. It follows that if the condition

$$\left(M_1^1N_1^1 + S_1^1T_1^1\right)\left[\left(P_1^1\right)^2 + \left(O_1^1\right)^2\right] + \left(Q_1^1P_1^1\right)\left[\left(N_1^1\right)^2 + \left(T_1^1\right)^2\right] \neq 0 \tag{17}$$

is satisfied, then

$$\mathrm{Re}\left[\left(\left.\frac{d\lambda_1}{d\tau_2}\right|_{\tau_2=\tau_2^0}\right)^{-1}\right] \neq 0.$$

Therefore, by Lemma 2.2 in [30] and Hopf bifurcation theory [31], we obtain the following theorem:

Theorem 3 *Suppose that* $\tau_1 = 0$, *and* $\tau_2 > 0$. *If equation* (14) *has positive roots and condition* (17) *is met, then*

(*i*) *when* $\tau_2 \in (0, \tau_2^0)$, E_0 *is locally asymptotically stable*;
(*ii*) *when* $\tau_2 > \tau_2^0$, E_0 *is unstable*;
(*iii*) *when* $\tau_2 = \tau_2^0$, *system* (1) *has a Hopf bifurcation at* E_0.

Case 3.2.3 If $\tau_1 > 0$, and $\tau_2 = 0$, then equations (7) and (13) become

$$\lambda^2 + \left(A_1^1 + C_0^1\right)\lambda + A_2^1 + C_1^1 + \left[B_0^1\lambda + \left(B_1^1 + D_0^1\right)\right]e^{-\lambda\tau_1} = 0, \tag{18}$$

and

$$\omega^4 + \left[\left(A_1^1 + C_0^1\right)^2 - 2\left(A_2^1 + C_1^1\right) - \left(B_0^1\right)^2\right]\omega^2 + \left(A_2^1 + C_1^1\right)^2 - \left(B_1^1 + D_0^1\right)^2 = 0, \tag{19}$$

respectively, where A_1^1, A_2^1, B_0^1, B_1^1, C_0^1, C_1^1, and D_0^1 are as defined in (7). Using similar argument as for Case 3.2.2, we have

$$\tau_1^j = \frac{1}{\omega_1^j}\left(\arccos\left[\frac{\bar{M}_1\bar{M}_3(\omega_1^j) + \bar{M}_2\bar{M}_4(\omega_1^j)}{\bar{M}_1^2 + \bar{M}_2^2}\right]\right), \quad j = 1, 2,$$
$$\tau_1^0 = \min_{j\in\{1,2\}}\left\{\tau_1^j\right\}, \qquad \omega_1^0 = \arg\min_{j\in\{1,2\}}\left\{\tau_1^j\right\},$$

where ω_1^1 and ω_1^2 are two positive roots of (19); $\bar{M}_1 = B_1^1 + D_0^1$; $\bar{M}_2 = B_0^1$; $\bar{M}_3(\omega_1^j) = (\omega_1^j)^2 - (A_2^1 + C_1^1)$; and $\bar{M}_4(\omega_1^j) = -(A_1^1 + C_0^1)\omega_1^j$. Moreover, we consider the root of equation (18) as $\lambda_2(\tau_1) = \xi_2(\tau_1) + i\omega_2(\tau_1)$ with $\xi_2(\tau_1^0) = 0$ and $\omega_2(\tau_1^0) = \omega_1^0$. Then, we have

$$\mathrm{Re}\left[\left(\frac{d\lambda_2}{d\tau_1}\bigg|_{\tau_1=\tau_1^0}\right)^{-1}\right] = \frac{(\bar{M}_1^1\bar{N}_1^1 + \bar{S}_1^1\bar{T}_1^1)[(\bar{P}_1^1)^2 + (\bar{O}_1^1)^2] + (\bar{Q}_1^1\bar{P}_1^1)[(\bar{N}_1^1)^2 + (\bar{T}_1^1)^2]}{[(\bar{N}_1^1)^2 + (\bar{T}_1^1)^2][(\bar{P}_1^1)^2 + (\bar{O}_1^1)^2]},$$

where $\bar{M}_1^1 = A_1^1 + C_0^1$; $\bar{S}_1^1 = 2\omega_1^0$; $\bar{N}_1^1 = (A_1^1 + C_0^1)(\omega_1^0)^2$; $\bar{T}_1^1 = (\omega_1^0)^3 - (A_2^1 + C_1^1)\omega_1^0$; $\bar{Q}_1^1 = B_0^1$; $\bar{P}_1^1 = -B_0^1(\omega_1^0)^2$; and $\bar{O}_1^1 = (B_1^1 + D_0^1)\omega_1^0$. Obviously, if condition

$$\left(\bar{M}_1^1\bar{N}_1^1 + \bar{S}_1^1\bar{T}_1^1\right)\left[\left(\bar{P}_1^1\right)^2 + \left(\bar{O}_1^1\right)^2\right] + \left(\bar{Q}_1^1\bar{P}_1^1\right)\left[\left(\bar{N}_1^1\right)^2 + \left(\bar{T}_1^1\right)^2\right] \neq 0 \tag{20}$$

is satisfied, then

$$\mathrm{Re}\left[\left(\frac{d\lambda_2}{d\tau_1}\bigg|_{\tau_1=\tau_1^0}\right)^{-1}\right] \neq 0.$$

Thus, we have the following theorem:

Theorem 4 *Suppose that* $\tau_2 = 0$, *and* $\tau_1 > 0$. *If equation* (19) *has positive roots and condition* (20) *is met, then*

(*i*) *when* $\tau_1 \in (0, \tau_1^0)$, E_0 *is locally asymptotically stable*;
(*ii*) *when* $\tau_1 > \tau_1^0$, E_0 *is unstable*;
(*iii*) *when* $\tau_1 = \tau_1^0$, *system* (1) *has a Hopf bifurcation at* E_0.

Case 3.2.4 If $\tau_1 > 0$, and $\tau_2 > 0$, then as shown in [32], it is difficult to directly analyze the Hopf bifurcation with two delays. Thus, further, we only discuss the Hopf bifurcation of equilibrium point for system (1) with one delay and the other delay lying in its stability region. Without loss of generality, we investigate the Hopf bifurcation at E_0 for system (1) with $\tau_1 > 0$ and $\tau_2 \in (0, \tau_2^0)$, where τ_2^0 is as given in Case 3.2.2. Let $\tau_2 \in (0, \tau_2^0)$ be arbitrary but fixed. Then, $\lambda = i\omega$ ($\omega > 0$) is a pure imaginary root of equation (7) if and only if

$$\begin{aligned} &-\omega^2 + A_1^1 i\omega + A_2^1 + \left(B_0^1 i\omega + B_1^1\right)\left(\cos(\omega\tau_1) - i\sin(\omega\tau_1)\right) + \left(C_0^1 i\omega + C_1^1\right) \\ &\quad \times \left[\cos(\omega\tau_2) - i\sin(\omega\tau_2)\right] + D_0^1\left[\cos\left(\omega(\tau_1+\tau_2)\right) - i\sin\left(\omega(\tau_1+\tau_2)\right)\right] = 0. \end{aligned} \tag{21}$$

Separating the real part from the imaginary part in (21) gives

$$\begin{cases} (B_0^1\omega - D_0^1\sin(\omega\tau_2))\sin(\omega\tau_1) + (B_1^1 + D_0^1\cos(\omega\tau_2))\cos(\omega\tau_1) \\ \quad = -[(-\omega^2 + A_2^1) + C_0^1\omega\sin(\omega\tau_2) + C_1^1\cos(\omega\tau_2)], \\ (B_0^1\omega - D_0^1\sin(\omega\tau_2))\cos(\omega\tau_1) - (B_1^1 + D_0^1\cos(\omega\tau_2))\sin(\omega\tau_1) \\ \quad = -(A_1^1\omega + C_0^1\omega\cos(\omega\tau_2) - C_1^1\sin(\omega\tau_2)). \end{cases} \tag{22}$$

By adding the squares of two equations in (22), we obtain

$$\omega^4 + l_1(\omega)\omega^3 + l_2(\omega)\omega^2 + l_3(\omega)\omega + l_4(\omega) = 0, \tag{23}$$

where $l_1(\omega) = -2C_0^1\sin(\omega\tau_2)$; $l_2(\omega) = (A_1^1)^2 - 2A_2^1 + (C_0^1)^2 - (B_0^1)^2 + 2(-C_1^1 + A_1^1C_0^1)\cos\omega\tau_2$; $l_3(\omega) = 2(A_2^1C_0^1 + B_0^1D_0^1 - A_1^1C_1^1)\sin(\omega\tau_2)$; and $l_4(\omega) = (A_2^1)^2 + (C_1^1)^2 - (B_1^1)^2 - (D_0^1)^2 + 2(A_2^1C_1^1 - B_1^1D_0^1)\cos\omega\tau_2$. Let

$$G_1(\omega) = \omega^4 + l_1(\omega)\omega^3 + l_2(\omega)\omega^2 + l_3(\omega)\omega + l_4(\omega). \tag{24}$$

Clearly, if $l_4(0) < 0$, then $G_1(0) < 0$. Besides, $\lim_{\omega\to+\infty} G_1(\omega) = +\infty$. Hence, equation (23) has at least one positive root denoted by $\tilde{\omega}_1$. Furthermore, substituting $\tilde{\omega}_1$ into (22) and solving the resulting equations, we have

$$\tilde{\tau}_1^k = \frac{1}{\tilde{\omega}_1}\left(\arccos\left[\frac{M_5(\tilde{\omega}_1)M_7(\tilde{\omega}_1) + M_6(\tilde{\omega}_1)M_8(\tilde{\omega}_1)}{M_5{}^2(\tilde{\omega}_1) + M_6{}^2(\tilde{\omega}_1)}\right] + 2k\pi\right), \quad k = 0, 1, 2, \ldots,$$

where $M_5(\tilde{\omega}_1) = (B_1^1 + D_0^1\cos(\tilde{\omega}_1\tau_2))$; $M_6(\tilde{\omega}_1) = (B_0^1\tilde{\omega}_1 - D_0^1\sin(\tilde{\omega}_1\tau_2))$; $M_7(\tilde{\omega}_1) = -[(-\tilde{\omega}_1^2 + A_2^1) + C_0^1\tilde{\omega}_1\sin(\tilde{\omega}_1\tau_2) + C_1^1\cos(\tilde{\omega}_1\tau_2)]$; and $M_8(\tilde{\omega}_1) = -(A_1^1\tilde{\omega}_1 + C_0^1\tilde{\omega}_1\cos(\tilde{\omega}_1\tau_2) - C_1^1\sin(\tilde{\omega}_1\tau_2))$. Obviously,

$$\lim_{k\to\infty} \tilde{\tau}_1^k = \infty.$$

Thus, we can define

$$\tilde{\omega}_1^0 = \arg\min\left\{\tilde{\tau}_1^0\right\}. \tag{25}$$

As discussed in Case 3.2.3, we consider the roots of equation (7) as a function of τ_1 and the root $\lambda_3(\tau_1) = \xi_3(\tau_1) + i\omega_3(\tau_1)$ of equation (7) such that

$$\xi_3\left(\tilde{\tau}_1^0\right) = 0, \quad \text{and} \quad \omega_3\left(\tilde{\tau}_1^0\right) = \tilde{\omega}_1^0.$$

Substituting $\lambda_3(\tau_1)$ into equation (7) and taking the derivative with respect to τ_1, we have

$$\left(\frac{d\lambda_3}{d\tau_1}\right)^{-1} = \frac{2\lambda_3 + A_1^1 + C_0^1 e^{-\lambda_3\tau_2} + (C_0^1\lambda_3 + C_1^1)e^{-\lambda_3\tau_2}(-\tau_2)}{-\lambda_3[(\lambda_3)^2 + A_1^1\lambda_3 + A_2^1 + (C_0^1\lambda_3 + C_1^1)e^{-\lambda_3\tau_2}]} + \frac{B_0^1 + D_0^1 e^{-\lambda_3\tau_2}(-\tau_2)}{\lambda_3[(B_0^1\lambda_3 + B_1^1) + D_0^1 e^{-\lambda_3\tau_2}]} - \frac{\tau_1}{\lambda_3}.$$

Then,

$$\mathrm{Re}\left[\left(\frac{d\lambda_3}{d\tau_1}\Big|_{\tau=\tilde{\tau}_1^0}\right)^{-1}\right] = \frac{(M_3^1N_3^1 + S_3^1T_3^1)[(P_3^1)^2 + (O_3^1)^2] + (Q_3^1P_3^1 + R_3^1O_3^1)[(N_3^1)^2 + (T_3^1)^2]}{[(N_3^1)^2 + (T_3^1)^2][(P_3^1)^2 + (O_3^1)^2]},$$

where $M_3^1 = A_1^1 + C_0^1\cos(\tilde{\omega}_1^0\tau_2) - \tau_2C_0^1\tilde{\omega}_1^0\sin(\tilde{\omega}_1^0\tau_2) - \tau_2C_1^1\cos(\tilde{\omega}_1^0\tau_2)$; $S_3^1 = 2\tilde{\omega}_1^0 - C_0^1\sin(\tilde{\omega}_1^0\tau_2) - \tau_2C_0^1\tilde{\omega}_1^0\cos(\tilde{\omega}_1^0\tau_2) + \tau_2C_1^1\sin(\tilde{\omega}_1^0\tau_2)$; $N_3^1 = -A_1^1(\tilde{\omega}_1^0)^2 - C_0^1(\tilde{\omega}_1^0)^2\cos(\tilde{\omega}_1^0\tau_2) + C_1^1\tilde{\omega}_1^0\sin(\tilde{\omega}_1^0\tau_2)$; $T_3^1 = -(\tilde{\omega}_1^0)^3 + A_2^1\tilde{\omega}_1^0 + C_0^1(\tilde{\omega}_1^0)^2\sin(\tilde{\omega}_1^0\tau_2) + C_1^1\tilde{\omega}_1^0\cos(\tilde{\omega}_1^0\tau_2)$; $Q_3^1 = B_0^1 - \tau_2^0D_0^1\cos(\tilde{\omega}_1^0\tau_2^0)$; $R_3^1 = \tau_2^0D_0^1\sin(\tilde{\omega}_1^0\tau_2^0)$; $P_3^1 = -B_0^1(\tilde{\omega}_1^0)^2 + D_0^1\cos(\tilde{\omega}_1^0\tau_2^0)$; and $O_3^1 = B_1^1\tilde{\omega}_1^0 - D_0^1\sin(\tilde{\omega}_1^0\tau_2^0)$. It follows that if the condition

$$\left(M_3^1N_3^1 + S_3^1T_3^1\right)\left[\left(P_3^1\right)^2 + \left(O_3^1\right)^2\right] + \left(Q_3^1P_3^1 + R_3^1O_3^1\right)\left[\left(N_3^1\right)^2 + \left(T_3^1\right)^2\right] \neq 0 \tag{26}$$

is satisfied, then

$$\mathrm{Re}\left[\left(\frac{d\lambda_3}{d\tau_1}\Big|_{\tau_1=\tilde{\tau}_1^0}\right)^{-1}\right] \neq 0.$$

As a result, by the Hopf bifurcation theory [31], we obtain the following theorem:

Theorem 5 *Suppose that* $\tau_1 > 0$, *and* $\tau_2 \in (0, \tau_2^0)$ *with* τ_2^0 *as defined in Case* 3.2.2. *If equation* (23) *has positive roots and condition* (26) *is met, then*

(*i*) *when* $\tau_1 \in (0, \tilde{\tau}_1^0)$, E_0 *is locally asymptotically stable*;

(*ii*) *when* $\tau_1 > \tilde{\tau}_1^0$, E_0 *is unstable*;

(*iii*) *when* $\tau_1 = \tilde{\tau}_1^0$, *system* (1) *has a Hopf bifurcation at* E_0.

3.3 Stability and Hopf bifurcation of endemic equilibrium point

The Jacobian matrix of the system (1) at E_1 is given by

$$J_{E_1} = \begin{pmatrix} -(Y+d) & -Y_1 & -Y_2 & -\frac{-\beta_1S^*E^* - \beta_2S^*I^*}{(N^*)^2} \\ Y & -(Y_3 - Y_1) & Y_2 & -\frac{\beta_1S^*E^* + \beta_2S^*I^*}{(N^*)^2} \\ 0 & \varepsilon e^{-\lambda\tau_1} & Y_4 & 0 \\ 0 & \gamma_2 & \gamma_1e^{-\lambda\tau_2} & -d \end{pmatrix}, \tag{27}$$

where $N^* = S^* + E^* + I^* + R^*$; $Y = \frac{\beta_1(N^* - S^*)E^*}{(N^*)^2} + \frac{\beta_2(N^* - S^*)I^*}{(N^*)^2}$; $Y_1 = \frac{\beta_1S^*N^* - \beta_1S^*E^* - \beta_2S^*I^*}{(N^*)^2}$; $Y_2 = \frac{\beta_2S^*N^* - \beta_2S^*I^* - \beta_1S^*E^*}{(N^*)^2}$; $Y_3 = \varepsilon e^{-\lambda\tau_1} + \gamma_2 + d$; and $Y_4 = -(\mu + d + \gamma_1e^{-\lambda\tau_2})$. For (27), one negative eigenvalue is given by $\lambda_1 = -d$. The other eigenvalues are determined by the following characteristic equation:

$$\lambda^3 + A_1^2\lambda^2 + A_2^2\lambda + A_3^2 + \left(B_0^2\lambda^2 + B_1^2\lambda + B_2^2\right)e^{-\lambda\tau_1} + \left(C_0^2\lambda^2 + C_1^2\lambda + C_2^2\right)e^{-\lambda\tau_2} + \left(D_0^2\lambda + D_1^2\right)e^{-\lambda(\tau_1+\tau_2)} = 0, \tag{28}$$

where $A_1^2 = (Y+d)+(\gamma_2+d)+(\mu+d)-Y_1$; $A_2^2 = (Y+d)(\gamma_2+d)+(Y+d)(\mu+d)+(\gamma_2+d)(\mu+d)-(\mu+2d)Y_1+\gamma_2\frac{\beta_1S^*E^*+\beta_2S^*I^*}{(N^*)^2}$; $A_3^2 = (Y+d)(\gamma_2+d)(\mu+d)-Y_1(\mu+d)d+\frac{\beta_1S^*E^*+\beta_2S^*I^*}{(N^*)^2}(\mu+d)\gamma_2$; $B_0^2=\varepsilon$; $B_1^2=(Y+d)\varepsilon+(\mu+d)\varepsilon-Y_2\varepsilon$; $B_2^2=(Y+d)(\mu+d)\varepsilon-\varepsilon dY_2$; $C_0^2=\gamma_1$; $C_1^2=(Y+d)\gamma_1+(\gamma_2+d)\gamma_1-Y_1\gamma_1$; $C_2^2=(Y+d)(\gamma_2+d)\gamma_1+\gamma_1\gamma_2\frac{\beta_1S^*E^*+\beta_2S^*I^*}{(N^*)^2}-\gamma_1 dY_1$; $D_0^2=\varepsilon\gamma_1$; and $D_1^2=\frac{\beta_1S^*E^*+\beta_2S^*I^*}{(N^*)^2}\varepsilon\gamma_1+(Y+d)\varepsilon\gamma_1$.

Now, we investigate the following cases for τ_1 and τ_2 at the endemic equilibrium point E_1.

Case 3.3.1 If $\tau_1=\tau_2=0$, then equation (28) turns to

$$\lambda^3+\left(A_1^2+B_0^2+C_0^2\right)\lambda^2+\left(A_2^2+B_1^2+C_1^2+D_0^2\right)\lambda+A_3^2+B_2^2+C_2^2+D_1^2=0. \tag{29}$$

Let

$$\begin{cases} a_0^2=1,\\ a_1^2=A_1^2+B_0^2+C_0^2\\ \quad =Y+\gamma_2+\mu+3d+\varepsilon+\gamma_1+\frac{\beta_1S^*E^*+\beta_2S^*I^*}{(N^*)^2}-\frac{\beta_1S^*N^*}{(N^*)^2},\\ a_2^2=A_2^2+B_1^2+C_1^2+D_0^2=(Y+d)(\varepsilon+\gamma_2+d)+(Y+d)(\mu+\gamma_1+d)\\ \quad +(\varepsilon+\gamma_2+d)(\mu+\gamma_1+d)+(\varepsilon+\gamma_2+\mu+\gamma_1+2d)\\ \quad +(\varepsilon+\gamma_2+\gamma_1+\mu+2d)\frac{\beta_1S^*E^*+\beta_2S^*I^*}{(N^*)^2}-(\gamma_1+\mu+2d)\\ \quad \times\frac{\beta_1S^*N^*}{(N^*)^2}-\varepsilon\frac{\beta_2S^*N^*}{(N^*)^2},\\ a_3^2=A_3^2+B_2^2+C_2^2+D_1^2=Y(\varepsilon+\gamma_2+d)(\mu+\gamma_1+d)+[d(\varepsilon+\mu\\ \quad +\gamma_1+d)+\varepsilon\gamma_1+(\mu+\gamma_1+d)\gamma_2]\frac{\beta_1S^*E^*+\beta_2S^*I^*}{(N^*)^2}. \end{cases}$$

Obviously,

$$a_1^2>Y+d+\mu+\gamma_1+d+\frac{\beta_1S^*E^*+\beta_2S^*I^*}{(N^*)^2},$$

and

$$a_2^2>Y(\varepsilon+\gamma_2+d)+(Y+d)(\mu+\gamma_1+d)+(\varepsilon+\gamma_2+d+\mu+\gamma_1+d)\times\frac{\beta_1S^*E^*+\beta_2S^*I^*}{(N^*)^2}.$$

Then, we have

$$a_1^2a_2^2>a_0^2a_3^2,\quad \text{and}\quad a_i^2>0,\quad i=0,1,2,3.$$

Recall that the positive endemic equilibrium point E_1 exists if and only if $R_0>1$. Thus, by the Routh-Hurwitz theorem [29], we have the following theorem:

Theorem 6 *Suppose that* $\tau_1=\tau_2=0$. *If* $R_0>1$, *then* E_1 *is locally asymptotically stable.*

Case 3.3.2 If $\tau_1=0$, and $\tau_2>0$, then equation (28) turns to

$$\begin{aligned}&\lambda^3+\left(A_1^2+B_0^2\right)\lambda^2+\left(A_2^2+B_1^2\right)\lambda+A_3^2+B_2^2\\ &\quad+\left[C_0^2\lambda^2+\left(C_1^2+D_0^2\right)\lambda+C_2^2+D_1^2\right]e^{-\lambda\tau_2}=0.\end{aligned} \tag{30}$$

To discuss the Hopf bifurcation of (30), we observe that $\lambda = i\omega$ ($\omega > 0$) is a pure imaginary root of the equation (30) if and only if

$$\begin{aligned} &-i\omega^3 - \left(A_1^2 + B_0^2\right)\omega^2 + \left(A_2^2 + B_1^2\right)i\omega + A_3^2 + B_2^2 \\ &\quad + \left[-C_0^2\omega^2 + \left(C_1^2 + D_0^2\right)i\omega + C_2^2 + D_1^2\right]\left(\cos(\omega\tau_2) - i\sin(\omega\tau_2)\right) = 0. \end{aligned} \tag{31}$$

Separating the real part from the imaginary part in (31) gives

$$\begin{cases} (A_1^2 + B_0^2)\omega^2 - (A_3^2 + B_2^2) = (-C_0^2\omega^2 + C_2^2 + D_1^2)\cos(\omega\tau_2) + (C_1^2 + D_0^2)\omega\sin(\omega\tau_2), \\ \omega^3 - (A_2^2 + B_1^2)\omega = -(-C_0^2\omega^2 + C_2^2 + D_1^2)\sin(\omega\tau_2) + (C_1^2 + D_0^2)\omega\cos(\omega\tau_2). \end{cases} \tag{32}$$

By adding the squares of two equations in (32), we obtain

$$\begin{aligned} &\omega^6 + \left[\left(A_1^2 + B_0^2\right)^2 - 2\left(A_2^2 + B_1^2\right) - \left(C_0^2\right)^2\right]\omega^4 + \left[\left(A_2^2 + B_1^2\right)^2 - 2\left(A_1^2 + B_0^2\right)\left(A_3^2\right.\right. \\ &\quad \left.\left. + B_2^2\right) - \left(C_1^2 + D_0^2\right)^2 + 2C_0^2\left(C_2^2 + D_1^2\right)\right]\omega^2 + \left(A_3^2 + B_2^2\right)^2 - \left(C_2^2 + D_1^2\right)^2 = 0. \end{aligned} \tag{33}$$

Let $z = \omega^2$, $h_{03} = (A_3^2 + B_2^2)^2 - (C_2^2 + D_1^2)^2$, $h_{13} = (A_2^2 + B_1^2)^2 - 2(A_1^2 + B_0^2)(A_3^2 + B_2^2) - (C_1^2 + D_0^2)^2 + 2C_0^2(C_2^2 + D_1^2)$ and $h_{23} = (A_1^2 + B_0^2)^2 - 2(A_2^2 + B_1^2) - (C_0^2)^2$. Then, (33) can be rewritten as

$$z^3 + h_{23}z^2 + h_{13}z + h_{03} = 0. \tag{34}$$

Without loss of generality, we assume that equation (34) has three positive roots denoted by $\bar{z}_j$, $j = 1, 2, 3$. Then, three positive roots of equation (33) are

$$\bar{\omega}_2^j = \sqrt{\bar{z}_j}, \quad j = 1, 2, 3. \tag{35}$$

Furthermore, substituting (35) into (32) and solving the resulting equations, we have

$$\bar{\tau}_2^{j,k} = \frac{1}{\bar{\omega}_2^j}\left(\arccos\left[\frac{(\hat{J} - \hat{F}C_0^2)(\bar{\omega}_2^j)^4 + (C_0^2\hat{I} + \hat{F}\hat{K} - \hat{H}\hat{J})(\bar{\omega}_2^j)^2 - \hat{I}\hat{K}}{\hat{J}^2(\bar{\omega}_2^j)^2 + (\hat{K} - C_0^2(\bar{\omega}_2^j)^2)^2}\right] + 2k\pi\right),$$

$$j = 1, 2, 3; \quad k = 0, 1, \ldots,$$

where $\hat{F} = A_1^2 + B_0^2$; $\hat{H} = A_2^2 + B_1^2$; $\hat{I} = A_3^2 + B_2^2$; $\hat{J} = C_1^2 + D_0^2$; and $\hat{K} = C_2^2 + D_1^2$. Clearly,

$$\lim_{k\to\infty} \bar{\tau}_2^{j,k} = \infty, \quad j = 1, 2, 3.$$

Thus, we can define

$$\bar{\tau}_2^0 = \min_{j\in\{1,2,3\}}\left\{\bar{\tau}_2^{j,0}\right\}, \quad \text{and} \quad \bar{\omega}_2^0 = \arg\min_{j\in\{1,2,3\}}\left\{\bar{\tau}_2^{j,0}\right\}. \tag{36}$$

Now, we consider the roots of equation (30) as a function of τ_2 and the root $\tilde{\lambda}_1(\tau_2) = \alpha_1(\tau_2) + i\tilde{\omega}_1(\tau_2)$ of equation (30) such that

$$\alpha_1\left(\bar{\tau}_2^0\right) = 0, \quad \text{and} \quad \tilde{\omega}_1\left(\bar{\tau}_2^0\right) = \bar{\omega}_2^0,$$

where $\bar{\tau}_2^0$ and $\bar{\omega}_2^0$ are as defined in (36). Substituting $\tilde{\lambda}_1(\tau_2)$ into equation (30) and taking the derivative with respect to τ_2, we have

$$\left(\frac{d\tilde{\lambda}_1}{d\tau_2}\right)^{-1} = \frac{3\tilde{\lambda}_1^2 + 2(A_1^2 + B_0^2)\tilde{\lambda}_1 + (A_2^2 + B_1^2)}{-\tilde{\lambda}_1[\tilde{\lambda}_1^3 + (A_1^2 + B_0^2)\tilde{\lambda}_1^2 + (A_2^2 + B_1^2)\tilde{\lambda}_1 + A_3^2 + B_2^2]} + \frac{2C_0^2\tilde{\lambda}_1 + C_1^2 + D_0^2}{\tilde{\lambda}_1[C_0^2\tilde{\lambda}_1^2 + (C_1^2 + D_0^2)\tilde{\lambda}_1 + C_2^2 + D_1^2]} - \frac{\tau_2}{\tilde{\lambda}_1}.$$

Then,

$$\mathrm{Re}\left[\left(\frac{d\tilde{\lambda}_1}{d\tau_2}\Big|_{\tau_2=\bar{\tau}_2^0}\right)^{-1}\right] = \frac{(M_1^2N_1^2 + S_1^2T_1^2)[(P_1^2)^2 + (O_1^2)^2] + (Q_1^2P_1^2 + R_1^2O_1^2)[(N_1^2)^2 + (T_1^2)^2]}{[(N_1^2)^2 + (T_1^2)^2][(P_1^2)^2 + (O_1^2)^2]},$$

where $M_1^2 = -3(\bar{\omega}_2^0)^2 + (A_2^2 + B_1^2)$, $S_1^2 = 2(A_1^2 + B_0^2)\bar{\omega}_2^0$, $N_1^2 = -(\bar{\omega}_2^0)^4 + (A_2^2 + B_1^2)(\bar{\omega}_2^0)^2$, $T_1^2 = (A_1^2 + B_0^2)(\bar{\omega}_2^0)^3 - (A_3^2 + B_2^2)\bar{\omega}_2^0$, $Q_1^2 = C_1^2 + D_0^2$, $R_1^2 = 2C_0^2\bar{\omega}_2^0$, $P_1^2 = -(C_1^2 + D_0^2)(\bar{\omega}_2^0)^2$, and $O_1^2 = -C_0^2(\bar{\omega}_2^0)^3 + (C_2^2 + D_1^2)\bar{\omega}_2^0$. It follows that if the condition

$$\left(M_1^2N_1^2 + S_1^2T_1^2\right)\left[\left(P_1^2\right)^2 + \left(O_1^2\right)^2\right] + \left(Q_1^2P_1^2 + R_1^2O_1^2\right)\left[\left(N_1^2\right)^2 + \left(T_1^2\right)^2\right] \neq 0 \tag{37}$$

is satisfied, then

$$\mathrm{Re}\left[\left(\frac{d\tilde{\lambda}_1}{d\tau_2}\Big|_{\tau_2=\bar{\tau}_2^0}\right)^{-1}\right] \neq 0.$$

Hence, by the Hopf bifurcation theory [31] and Lemma 2.1 in [33], we can obtain the following theorem:

Theorem 7 *Suppose that* $\tau_1 = 0$, *and* $\tau_2 > 0$. *If equation* (34) *has positive roots and condition* (37) *is met, then*

(*i*) *when* $\tau_2 \in (0, \bar{\tau}_2^0)$, E_1 *is locally asymptotically stable*;
(*ii*) *when* $\tau_2 > \bar{\tau}_2^0$, E_1 *is unstable*;
(*iii*) *when* $\tau_2 = \bar{\tau}_2^0$, *system* (1) *has a Hopf bifurcation at* E_1.

Case 3.3.3 If $\tau_1 > 0$, and $\tau_2 = 0$, then equations (28) and (33) become

$$\begin{aligned}&\lambda^3 + \left(A_1^2 + C_0^2\right)\lambda^2 + \left(A_2^2 + C_1^2\right)\lambda + A_3^2 + C_2^2\\ &\quad + \left[B_0^2\lambda^2 + \left(B_1^2 + D_0^2\right)\lambda + B_2^2 + D_1^2\right]e^{-\lambda\tau_1} = 0.\end{aligned} \tag{38}$$

and

$$\begin{aligned}&\omega^6 + \left[\left(A_1^2 + C_0^2\right)^2 - 2\left(A_2^2 + C_1^2\right) - \left(B_0^2\right)^2\right]\omega^4 + \left[\left(A_2^2 + C_1^2\right)^2 - 2\left(A_1^2 + C_0^2\right)\left(A_3^2\right.\right.\\ &\quad \left.\left. + C_2^2\right) - \left(B_1^2 + D_0^2\right)^2 + 2B_0^2\left(B_2^2 + D_1^2\right)\right]\omega^2 + \left(A_3^2 + C_2^2\right)^2 - \left(B_2^2 + D_1^2\right)^2 = 0,\end{aligned} \tag{39}$$

respectively, where A_1^2, A_2^2, A_3^2, B_0^2, B_1^2, B_2^2, C_0^2, C_1^2, C_2^2, D_0^2, and D_1^2 are as defined in (28). Using similar argument as given for Case 2.2.3, we have

$$\bar{\tau}_1^j = \frac{1}{\bar{\omega}_2^j}\left(\arccos\left[\frac{(\bar{J}-\bar{F}B_0^2)(\bar{\omega}_1^j)^4 + (B_0^2\bar{I}+\bar{F}\bar{K}-\bar{H}\bar{J})(\bar{\omega}_1^j)^2 - \bar{I}\bar{K}}{\bar{J}^2(\bar{\omega}_1^j)^2 + (\bar{K}-B_0^2(\bar{\omega}_1^j)^2)^2}\right]\right),$$

$j = 1, 2, 3,$

$$\bar{\tau}_1^0 = \min_{j\in\{1,2,3\}}\{\bar{\tau}_1^j\}, \qquad \bar{\omega}_1^0 = \arg\min_{j\in\{1,2,3\}}\{\bar{\tau}_1^j\},$$

where $\bar{\omega}_1^1$, $\bar{\omega}_1^2$, and $\bar{\omega}_1^3$ are three positive roots of (39); $\bar{F} = A_1^2 + C_0^2$; $\bar{H} = A_2^2 + C_1^2$; $\bar{I} = A_3^2 + C_2^2$; $\bar{J} = B_1^2 + D_0^2$; and $\bar{K} = B_2^2 + D_1^2$. Furthermore, we consider the root of equation (38) as $\tilde{\lambda}_2(\tau_1) = \alpha_2(\tau_1) + i\tilde{\omega}_2(\tau_1)$ with $\alpha_2(\bar{\tau}_1^0) = 0$ and $\tilde{\omega}_2(\bar{\tau}_1^0) = \bar{\omega}_1^0$. Then, we have

$$\begin{aligned}&\mathrm{Re}\left[\left(\frac{d\tilde{\lambda}_2}{d\tau_1}\bigg|_{\tau_1=\bar{\tau}_1^0}\right)^{-1}\right]\\ &\quad= \frac{(\bar{M}_1^2\bar{N}_1^2 + \bar{S}_1^2\bar{T}_1^2)[(\bar{P}_1^2)^2 + (\bar{O}_1^2)^2] + (\bar{Q}_1^2\bar{P}_1^2 + \bar{R}_1^2\bar{O}_1^2)[(\bar{N}_1^2)^2 + (\bar{T}_1^2)^2]}{[(\bar{N}_1^2)^2 + (\bar{T}_1^2)^2][(\bar{P}_1^2)^2 + (\bar{O}_1^2)^2]},\end{aligned}$$

where $\bar{M}_1^2 = -3(\bar{\omega}_1^0)^2 + (A_2^2 + C_1^2)$, $\bar{S}_1^2 = 2(A_1^2 + C_0^2)\bar{\omega}_1^0$, $\bar{N}_1^2 = -(\bar{\omega}_1^0)^4 + (A_2^2 + C_1^2)(\bar{\omega}_1^0)^2$, $\bar{T}_1^2 = (A_1^2 + C_0^2)(\bar{\omega}_1^0)^3 - (A_3^2 + C_2^2)\bar{\omega}_1^0$, $\bar{Q}_1^2 = B_1^2 + D_0^2$, $\bar{R}_1^2 = 2B_0^2\bar{\omega}_1^0$, $\bar{P}_1^2 = -(B_1^2 + D_0^2)(\bar{\omega}_1^0)^2$, and $\bar{O}_1^2 = -B_0^2(\bar{\omega}_1^0)^3 + (B_2^2 + D_1^2)\bar{\omega}_1^0$. Clearly, if condition

$$(\bar{M}_1^2\bar{N}_1^2 + \bar{S}_1^2\bar{T}_1^2)\left[(\bar{P}_1^2)^2 + (\bar{O}_1^2)^2\right] + (\bar{Q}_1^2\bar{P}_1^2 + \bar{R}_1^2\bar{O}_1^2)\left[(\bar{N}_1^2)^2 + (\bar{T}_1^2)^2\right] \neq 0 \tag{40}$$

is satisfied, then

$$\mathrm{Re}\left[\left(\frac{d\tilde{\lambda}_2}{d\tau_1}\bigg|_{\tau_1=\bar{\tau}_1^0}\right)^{-1}\right] \neq 0.$$

Thus, we have the following theorem:

Theorem 8 *Suppose that* $\tau_1 > 0$, *and* $\tau_2 = 0$. *If equation* (39) *has positive roots and condition* (40) *is met, then*

(*i*) *when* $\tau_1 \in (0, \bar{\tau}_1^0)$, E_1 *is locally asymptotically stable*;

(*ii*) *when* $\tau_1 > \bar{\tau}_1^0$, E_1 *is unstable*;

(*iii*) *when* $\tau_1 = \bar{\tau}_1^0$, *system* (1) *has a Hopf bifurcation at* E_1.

Case 3.3.4 If $\tau_1 > 0$, and $\tau_2 > 0$, then using the similar discussion as for Case 3.2.4, we consider the Hopf bifurcation of E_1 for the system (1) with $\tau_1 > 0$ and $\tau_2 \in (0, \bar{\tau}_2^0)$, where $\bar{\tau}_2^0$ as given in Case 3.3.2. Let $\tau_2 \in (0, \bar{\tau}_2^0)$ be arbitrary but fixed. Then, $\lambda = i\omega$ ($\omega > 0$) is a pure imaginary root of the equation (28) if and only if

$$\begin{aligned}&-i\omega^3 - A_1^2\omega^2 + A_2^2 i\omega + A_3^2 + \left(-B_0^2\omega^2 + B_1^2 i\omega + B_2^2\right)\left[\cos(\omega\tau_1)\right.\\ &\quad\left. - i\sin(\omega\tau_1)\right] + \left(-C_0^2\omega^2 + C_1^2 i\omega + C_2^2\right)\left[\cos(\omega\tau_2) - i\sin(\omega\tau_2)\right]\\ &\quad + \left(D_0^2 i\omega + D_1^2\right)\left[\cos\left(\omega(\tau_1+\tau_2)\right) - i\sin\left(\omega(\tau_1+\tau_2)\right)\right] = 0.\end{aligned} \tag{41}$$

Separating the real part from the imaginary part in (41) gives

$$\begin{cases} A_1^2\omega^2 - A_3^2 - (-C_0^2\omega^2 + C_2^2)\cos(\omega\tau_2) - C_1^2\omega\sin(\omega\tau_2) \\ \quad = (-B_0^2\omega^2 + B_2^2 + D_1^2\cos(\omega\tau_2) + D_0^2\omega\sin(\omega\tau_2))\cos(\omega\tau_1) \\ \qquad + (B_1^2\omega - D_1^2\sin(\omega\tau_2) + D_0^2\omega\cos(\omega\tau_2))\sin(\omega\tau_1), \\ \omega^3 - A_2^2\omega + (-C_0^2\omega^2 + C_2^2)\sin(\omega\tau_2) - C_1^2\omega\cos(\omega\tau_2) \\ \quad = -(-B_0^2\omega^2 + B_2^2 + D_1^2\cos(\omega\tau_2) + D_0^2\omega\sin(\omega\tau_2))\sin(\omega\tau_1) \\ \qquad + (B_1^2\omega - D_1^2\sin(\omega\tau_2) + D_0^2\omega\cos(\omega\tau_2))\cos(\omega\tau_1). \end{cases} \tag{42}$$

By adding the squares of two equations in (42), we obtain

$$\omega^6 + \bar{l}_1(\omega)\omega^5 + \bar{l}_2(\omega)\omega^4 + \bar{l}_3(\omega)\omega^3 + \bar{l}_4(\omega)\omega^2 + \bar{l}_5(\omega)\omega + \bar{l}_6(\omega) = 0, \tag{43}$$

where $\bar{l}_1(\omega) = -2C_0^2\sin(\omega\tau_2)$; $\bar{l}_2(\omega) = (A_1^2)^2 - 2A_2^2 + (C_0^2)^2 - (B_0^2)^2 + 2(A_1^2C_0^2 - C_1^2)\cos(\omega\tau_2)$; $\bar{l}_3(\omega) = 2(C_2^2 + A_2^2C_0^2 - A_1^2C_1^2 + B_0^2D_0^2)\sin(\omega\tau_2)$; $\bar{l}_4(\omega) = (A_2^2)^2 + (C_1^2)^2 + 2B_0^2B_2^2 - 2A_1^2A_3^2 - 2C_0^2C_2^2 - (B_1^2)^2 - (D_0^2)^2 - 2(A_1^2C_2^2 - A_2^2C_1^2 + A_3^2C_0^2 + B_1^2D_0^2 - B_0^2D_1^2)\cos(\omega\tau_2)$; $\bar{l}_5(\omega) = 2(A_3^2C_1^2 - A_2^2C_2^2 - B_2^2D_0^2 + B_1^2D_1^2)\sin(\omega\tau_2)$; and $\bar{l}_6(\omega) = (C_2^2)^2 + (A_3^2)^2 - (B_2^2)^2 - (D_1^2)^2 + (2A_3^2C_2^2 - 2B_2^2D_1^2)\cos(\omega\tau_2)$. Let

$$G_2(\omega) = \omega^6 + \bar{l}_1(\omega)\omega^5 + \bar{l}_2(\omega)\omega^4 + \bar{l}_3(\omega)\omega^3 + \bar{l}_4(\omega)\omega^2 + \bar{l}_5(\omega)\omega + \bar{l}_6(\omega). \tag{44}$$

Obviously, if $\bar{l}_6(0) < 0$, then $G_2(0) < 0$. In addition, $\lim_{\omega\to+\infty} G_2(\omega) = +\infty$. Hence, equation (43) has at least one positive root denoted by $\hat{\omega}_1$. Furthermore, substituting $\hat{\omega}_1$ into (43) and solving the resulting equations, we have

$$\hat{\tau}_1^k = \frac{1}{\hat{\omega}_1}\left(\arccos\left[\frac{M_9(\hat{\omega}_1)M_{11}(\hat{\omega}_1) + M_{10}(\hat{\omega}_1)M_{12}(\hat{\omega}_1)}{M_9{}^2(\hat{\omega}_1) + M_{10}{}^2(\hat{\omega}_1)}\right] + 2k\pi\right), \quad k = 0, 1, \ldots,$$

where $M_9(\hat{\omega}_1) = -B_0^2(\hat{\omega}_1)^2 + B_2^2 + D_1^2\cos(\hat{\omega}_1\tau_2) + D_0^2\hat{\omega}_1\sin(\hat{\omega}_1\tau_2)$; $M_{10}(\hat{\omega}_1) = B_1^2\hat{\omega}_1 - D_1^2\sin(\hat{\omega}_1\tau_2) + D_0^2\hat{\omega}_1\cos(\hat{\omega}_1\tau_2)$; $M_{11}(\hat{\omega}_1) = A_1^2(\hat{\omega}_1)^2 - A_3^2 - (-C_0^2(\hat{\omega}_1)^2 + C_2^2)\cos(\hat{\omega}_1\tau_2) - C_1^2\hat{\omega}_1\sin(\hat{\omega}_1\tau_2)$; and $M_{12}(\hat{\omega}_1) = (\hat{\omega}_1)^3 - A_2^2\hat{\omega}_1 + (-C_0^2(\hat{\omega}_1)^2 + C_2^2)\sin(\hat{\omega}_1\tau_2) - C_1^2\hat{\omega}_1\cos(\hat{\omega}_1\tau_2)$. Clearly,

$$\lim_{k\to\infty} \hat{\tau}_1^k = \infty.$$

Thus, we can define

$$\hat{\omega}_1^0 = \arg\min\{\hat{\tau}_1^0\}. \tag{45}$$

Next, we consider the roots of equation (28) as a function of τ_1 and the root $\tilde{\lambda}_3(\tau_1) = \alpha_3(\tau_1) + i\tilde{\omega}_3(\tau_1)$ of equation (28) such that

$$\alpha_3(\hat{\tau}_1^0) = 0, \quad \text{and} \quad \tilde{\omega}_3(\hat{\tau}_1^0) = \hat{\omega}_1^0.$$

Substituting $\tilde{\lambda}_3(\tau_1)$ into equation (28) and taking the derivative with respect to τ_1, we have

$$\begin{aligned}&\left(\frac{d\tilde{\lambda}_3}{d\tau_1}\right)^{-1}\\&= \frac{3(\tilde{\lambda}_3)^2 + 2A_1^2\tilde{\lambda}_3 + A_2^2 + (2C_0^2\tilde{\lambda}_3 + C_1^2)e^{-\tilde{\lambda}_3\tau_2} - \tau_2(C_0^2(\tilde{\lambda}_3)^2 + C_1^2\tilde{\lambda}_3 + C_2^2)e^{-\tilde{\lambda}_3\tau_2}}{-\tilde{\lambda}_3[(\tilde{\lambda}_3)^3 + A_1^2(\tilde{\lambda}_3)^2 + A_2^2\tilde{\lambda}_3 + A_3^2 + (C_0^2(\tilde{\lambda}_3)^2 + C_1^2\tilde{\lambda}_3 + C_2^2)e^{-\tilde{\lambda}_3\tau_2}]}\\&\quad + \frac{2B_0^2\tilde{\lambda}_3 + B_1^2 + D_0^2e^{-\tilde{\lambda}_3\tau_2} - \tau_2(D_0^2\tilde{\lambda}_3 + D_1^2)e^{-\tilde{\lambda}_3\tau_2}}{\tilde{\lambda}_3[B_0^2(\tilde{\lambda}_3)^2 + B_1^2\tilde{\lambda}_3 + B_2^2 + (D_0^2\tilde{\lambda}_3 + D_1^2)e^{-\tilde{\lambda}_3\tau_2}]} - \frac{\tau_1}{\tilde{\lambda}_3}.\end{aligned}$$

Then,

$$\operatorname{Re}\left[\left(\frac{d\tilde{\lambda}_3}{d\tau_1}\Big|_{\tau_1=\hat{\tau}_1^0}\right)^{-1}\right] = \frac{(M_3^2N_3^2 + S_3^2T_3^2)[(P_3^2)^2 + (O_3^2)^2] + (Q_3^2P_3^2 + R_3^2O_3^2)[(N_3^2)^2 + (T_3^2)^2]}{[(N_3^2)^2 + (T_3^2)^2][(P_3^2)^2 + (O_3^2)^2]},$$

where $M_3^2 = -3(\hat{\omega}_1^0)^2 + A_2^2 + 2C_0^2\hat{\omega}_1^0\sin(\hat{\omega}_1^0\tau_2) + C_1^2\cos(\hat{\omega}_1^0\tau_2) - \tau_2(-C_0^2(\hat{\omega}_1^0)^2 + C_2^2)\cos(\hat{\omega}_1^0\tau_2) - \tau_2C_1^2\hat{\omega}_1^0\sin(\hat{\omega}_1^0\tau_2)$; $S_3^2 = 2A_1^2\hat{\omega}_1^0 + 2C_0^2\hat{\omega}_1^0\cos(\hat{\omega}_1^0\tau_2) - C_1^2\sin(\hat{\omega}_1^0\tau_2) + \tau_2(-C_0^2(\hat{\omega}_1^0)^2 + C_2^2)\times\sin(\hat{\omega}_1^0\tau_2) - \tau_2C_1^2\hat{\omega}_1^0\cos(\hat{\omega}_1^0\tau_2)$; $N_3^2 = -(\hat{\omega}_1^0)^4 + A_2^2(\hat{\omega}_1^0)^2 + (C_0^2(\hat{\omega}_1^0)^3 - C_2^2\hat{\omega}_1^0)\sin(\hat{\omega}_1^0\tau_2) + C_1^2(\hat{\omega}_1^0)^2\cos(\hat{\omega}_1^0\tau_2)$; $T_3^2 = A_1^2(\hat{\omega}_1^0)^3 - A_3^2\hat{\omega}_1^0 + (C_0^2(\hat{\omega}_1^0)^3 - C_2^2\hat{\omega}_1^0)\cos(\hat{\omega}_1^0\tau_2) - C_1^2(\hat{\omega}_1^0)^2\sin(\hat{\omega}_1^0\tau_2)$; $Q_3^2 = B_1^2 + D_0^2\cos(\hat{\omega}_1^0\tau_2) - \tau_2D_0^2\hat{\omega}_1^0\sin(\hat{\omega}_1^0\tau_2) - \tau_2D_1^2\cos(\hat{\omega}_1^0\tau_2)$; $R_3^2 = 2B_0^2\hat{\omega}_1^0 - D_0^2\sin(\hat{\omega}_1^0\tau_2) - \tau_2D_0^2\hat{\omega}_1^0\cos(\hat{\omega}_1^0\tau_2) + \tau_2D_1^2\sin(\hat{\omega}_1^0\tau_2)$; $P_3^2 = -B_1^2(\hat{\omega}_1^0)^2 - D_0^2(\hat{\omega}_1^0)^2\cos(\hat{\omega}_1^0\tau_2) + D_1^2\hat{\omega}_1^0\sin(\hat{\omega}_1^0\tau_2)$; and $O_3^2 = -B_0^2(\hat{\omega}_1^0)^3 + B_2^2\hat{\omega}_1^0 + D_0^2(\hat{\omega}_1^0)^2\sin(\hat{\omega}_1^0\tau_2) + D_1^2\hat{\omega}_1^0\cos(\hat{\omega}_1^0\tau_2)$. Furthermore, if condition

$$\left(M_3^2N_3^2 + S_3^2T_3^2\right)\left[\left(P_3^2\right)^2 + \left(O_3^2\right)^2\right] + \left(Q_3^2P_3^2 + R_3^2O_3^2\right)\left[\left(N_3^2\right)^2 + \left(T_3^2\right)^2\right] \neq 0 \tag{46}$$

is satisfied, then

$$\operatorname{Re}\left[\left(\frac{d\tilde{\lambda}_3}{d\tau_1}\Big|_{\tau_1=\hat{\tau}_1^0}\right)^{-1}\right] \neq 0.$$

Thus, by the Hopf bifurcation theory [31], we can obtain the following theorem:

Theorem 9 *Suppose that* $\tau_1 > 0$, *and* $\tau_2 \in (0, \bar{\tau}_2^0)$ *with* $\bar{\tau}_2^0$ *as defined in Case* 3.3.2. *If equation* (43) *has positive roots and condition* (46) *is met, then*

(*i*) *when* $\tau_1 \in (0, \hat{\tau}_1^0)$, E_1 *is locally asymptotically stable*;

(*ii*) *when* $\tau_1 > \hat{\tau}_1^0$, E_1 *is unstable*;

(*iii*) *when* $\tau_1 = \hat{\tau}_1^0$, *system* (1) *has a Hopf bifurcation at* E_1.

4 Delay optimal control problem

In this section, we will consider the delay optimal control problem in the COVID-19 epidemic and will derive the corresponding necessary optimality conditions.

The outbreak of the COVID-19 epidemic can be controlled by two interventions: (i) reduction and suppression of social contact through masking, home isolation, etc. and (ii) pharmacological interventions, leading to the use of novel treatments that minimize mortality and shorten hospital stays. Let $u_1(t)$ and $u_2(t)$ be the social contact and the pharmaceutical intervention, respectively. Then, the controlled SEIR model in the COVID-19

virus transmission can be formulated as:

$$\begin{cases} \dot{S}(t) = \Lambda - \frac{\beta_1(1-u_1(t))S(t)E(t)}{N(t)} - \frac{\beta_2(1-u_1(t))S(t)I(t)}{N(t)} - dS(t), \\ \dot{E}(t) = \frac{\beta_1(1-u_1(t))S(t)E(t)}{N(t)} + \frac{\beta_2(1-u_1(t))S(t)I(t)}{N(t)} - \varepsilon E(t-\tau_1) \\ \qquad - (\gamma_2 + d)E(t), \qquad t \in [0,T], \\ \dot{I}(t) = \varepsilon E(t-\tau_1) - \gamma_1(1+u_2(t))I(t-\tau_2) - (\mu + d)I(t), \\ \dot{R}(t) = \gamma_1(1+u_2(t))I(t-\tau_2) + \gamma_2 E(t) - dR(t), \end{cases} \tag{47}$$

where $T > 0$ is a given terminal time. It should be noted that the suppression of social contacts is generally costly, and it will result in economy recession. Pharmacological intervention is also expensive because it requires extensive clinical trials prior to experimental treatment. Therefore, we assume that

$$0 \le u_i(t) \le u_i^{\max}, \quad i = 1,2, t \ge 0, \tag{48}$$

where $u_i^{\max}$ (≤ 1), $i = 1,2$, are the upper bounds for controls $u_i(t)$. Let $\mathcal{U}$ be the set of all Borel measurable functions $u_i : [0,T] \to \mathbb{R}$, $i = 1,2$, satisfying constraint (48).

Let $x(t) = (S(t), E(t), I(t), R(t))^\top$, $u(t) = (u_1(t), u_2(t))^\top$, and the right-hand side of system (47) be $\tilde{f}(x(t), x(t-\tau_1), x(t-\tau_2), u(t))$. Then, system (47) with the condition (2) in a finite time horizon $[-\tau, T]$ can be rewritten as

$$\begin{cases} \dot{x}(t) = \tilde{f}(x(t), x(t-\tau_1), x(t-\tau_2), u(t)), & t \in [0,T], \\ x(t) = \varphi(t), & t \in [-\tau, 0], \end{cases} \tag{49}$$

where $\varphi(t) = (\varphi_1(t), \varphi_2(t), \varphi_3(t), \varphi_4(t))^\top$ is the initial condition.

During the COVID-19 spread, social contacts can be mitigated and suppressed by non-pharmacological interventions, such as wearing masks, maintaining social distancing, testing and isolation, and closing businesses, while the length of hospital stay can be minimized by pharmacological interventions and using new treatment modalities. Thus, using both non-pharmacological and pharmacological interventions as the control strategies, our goal is to maximize the number of recovered individuals at the terminal time, as well as to minimize the number of exposed and infected individuals during the time horizon, and the system cost of control measures. Therefore, the cost function in controlling the COVID-19 epidemic can be stated as

$$J(u) = -q_1 x_4(T) + \frac{1}{2}\int_0^T \left[q_2 x_2^2(t) + q_3 x_3^2(t) + r_1 u_1^2(t) + r_2 u_2^2(t)\right] dt, \tag{50}$$

where $q_i > 0$, $i = 1,2,3$, $r_1 > 0$ and $r_2 > 0$ are weighting coefficients. As a result, we propose the following delay optimal control problem:

$$\text{(DOCP)} \quad \min \quad J(u)$$
$$\text{s.t.} \quad \begin{cases} \dot{x}(t) = \tilde{f}(x(t), x(t-\tau_1), x(t-\tau_2), u(t)), & t \in [0,T], \\ x(t) = \varphi(t), & t \in [-\tau, 0], \end{cases}$$
$$u \in \mathcal{U}.$$

To solve Problem (DOCP), we establish the following necessary optimality conditions.

Theorem 10 *Let $u^* \in \mathcal{U}$ be the optimal control of Problem (DOCP), and let $x^* = x(\cdot|u^*)$ be the corresponding solution of system (49). Then, there exists a costate vector $\lambda^*(t) = (\lambda_1^*(t), \lambda_2^*(t), \ldots, \lambda_4^*(t))^\top$ satisfying*

$$\begin{cases} \dot{\lambda}_1^*(t) = \lambda_1^*(t)(W_1 + W_2 + d) - \lambda_2^*(t)(W_1 + W_2), \\ \dot{\lambda}_2^*(t) = -q_2 x_2^*(t) + \lambda_1^*(t)(W_3 - W_5) - \lambda_2^*(t)(W_3 - W_5 - \gamma_2 - d) \\ \qquad + \lambda_2^*(t+\tau_1)\varepsilon - \lambda_3^*(t+\tau_1)\varepsilon - \lambda_4^*\gamma_2, & t \in [0, T], \\ \dot{\lambda}_3^*(t) = -q_3 x_3^*(t) + \lambda_1^*(t)(W_4 - W_6) - \lambda_2^*(t)(W_4 - W_6) \\ \qquad + \lambda_3^*(t+\tau_2)\gamma_1(1 + u_2^*(t)) + \lambda_3^*(t)(\mu + d) - \lambda_4^*(t+\tau_2)\gamma_1(1 + u_2^*(t)), \\ \dot{\lambda}_4^*(t) = -\lambda_1^*(W_5 + W_6) + \lambda_2^*(W_5 + W_6) + \lambda_4^* d, \end{cases}$$

with the conditions

$$\lambda(T) = (0, 0, 0, -q_1)^\top,$$

$$\lambda(t) = (0, 0, 0, 0)^\top, \quad t > T,$$

where $\bar{x}^*(t) = x_1^*(t) + x_2^*(t) + x_3^*(t) + x_4^*(t)$; $W_1 = \frac{\beta_1 x_2^*(t)(1-u_1^*(t))(\bar{x}^*(t)-x_1^*(t))}{(\bar{x}^*(t))^2}$; $W_2 = \frac{\beta_2 x_3^*(t)(1-u_1^*(t))(\bar{x}^*(t)-x_1^*(t))}{(\bar{x}^*(t))^2}$; $W_3 = \frac{\beta_1 x_1^*(t)(1-u_1^*(t))(\bar{x}^*(t)-x_2^*(t))}{(\bar{x}^*(t))^2}$; $W_4 = \frac{\beta_2 x_1^*(t)(1-u_1^*(t))(\bar{x}^*(t)-x_3^*(t))}{(\bar{x}^*(t))^2}$; $W_5 = \frac{\beta_2(1-u_1^*(t))x_1^*(t)x_3^*(t)}{(\bar{x}^*(t))^2}$; *and* $W_6 = \frac{\beta_1(1-u_1^*(t))x_1^*(t)x_2^*(t)}{(\bar{x}^*(t))^2}$. *Furthermore, the optimal control u^* can be expressed as*

$$\begin{cases} u_1^*(t) = \min(\max(\frac{(\lambda_2^*(t)-\lambda_1^*(t))(x_1^*(t)x_2^*(t)+x_1^*(t)x_3^*(t))}{\bar{x}^*(t)r_1}, 0), u_1^{\max}), \\ u_2^*(t) = \min(\max(\frac{(\lambda_3^*(t)-\lambda_4^*(t))x_3^*(t-\tau_2)}{r_2}, 0), u_2^{\max}). \end{cases}$$

Proof Using proof similar to Theorem 1 in [34], we can complete the proof. □

5 Numerical simulations

In this section, we will carry out some numerical simulations to verify the stability and the Hopf bifurcation of equilibrium points in Sect. 3. Moreover, Problem (DOCP) will be solved based on the derived necessary optimality conditions in Sect. 4.

5.1 Numerical simulations of stability and Hopf bifurcation

In numerical simulations, two sets of parameter values for system (1) are chosen (Table 1). In addition, the initial condition is chosen as $\varphi(t) = (99999, 1, 0, 0)^\top$ for $t \in [-\tau, 0]$. For the first set of parameter values (i.e., the second row in Table 1), we obtain $R_0 = 0.7037(< 1)$. In this case, system (1) has a unique disease-free equilibrium point $E_0 = (30, 0, 0, 0)$. For $\tau_1 = \tau_2 = 0$, we have $a_0^1 = 1$, $a_1^1 = 1.65$, $a_2^1 = 0.32$ and $a_3^1 = 0$. Obviously, $a_1^1 a_2^1 > a_0^1 a_3^1$ and E_0

Table 1 Two sets parameter values in the simulations

Parameters	β_1	β_2	Λ	d	γ_1	γ_2	μ	ε
First set of values	0.5	0.3	1.5	0.05	0.55	0.1	0.2	1.2
Second set of values	1	0.3	0.5	0.05	0.5	0.01	0.2	1.2

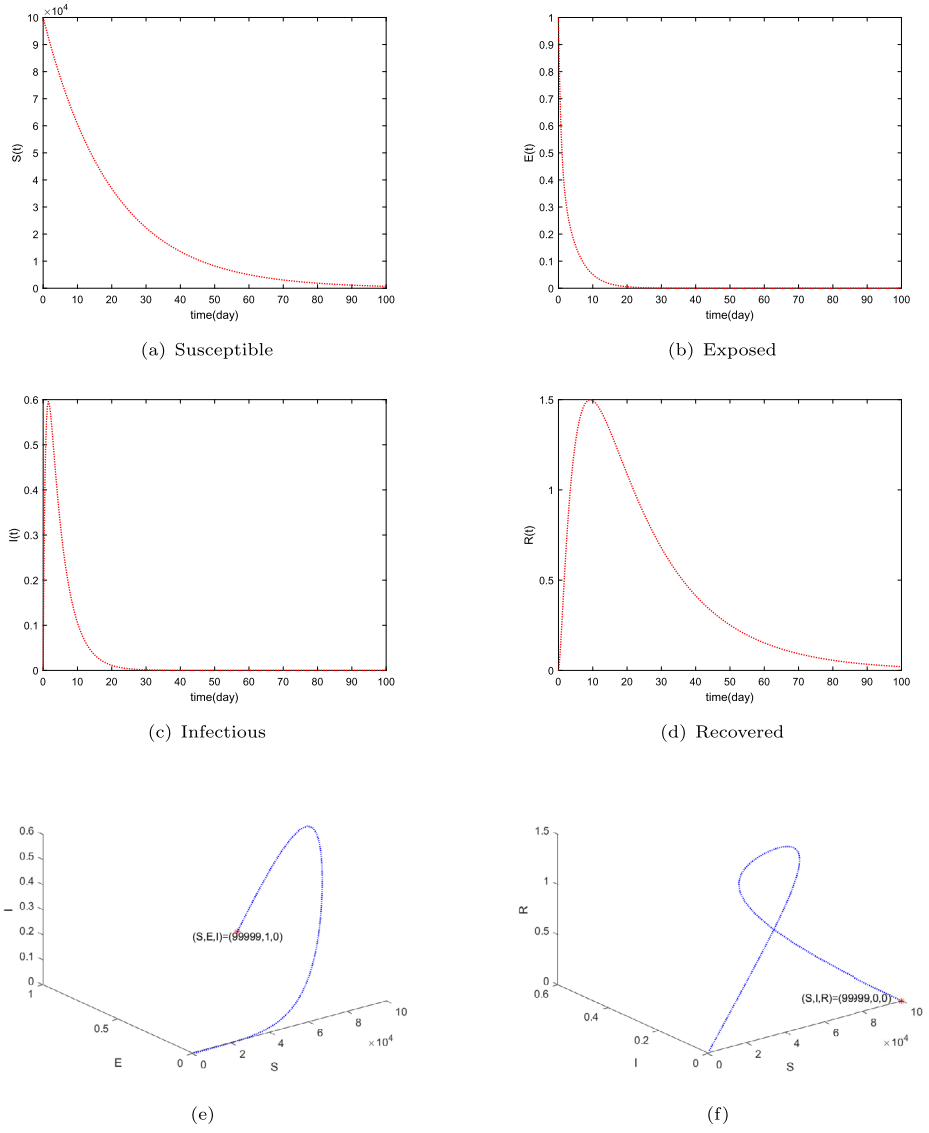

Figure 2 When $\tau_1 = \tau_2 = 0$, E_0 is asymptotically stable

is locally stable from Theorem 2 (Fig. 2). For $\tau_1 = 0$ and $\tau_2 > 0$, we obtain $\omega_2^0 = 0.3820$ and $\tau_2^0 = 3.8658$. As shown in Theorem 3, E_0 is asymptotically stable when $\tau_2 \in (0, 3.8658)$, and the Hopf bifurcation occurs when $\tau_2 = 3.8658$, which are illustrated in Figs. 3 and 4. For $\tau_1 > 0$ and $\tau_2 = 0$, we obtain $\omega_1^0 = 0.9840$ and $\tau_1^0 = 1.4683$. The corresponding asymptotic stability and the Hopf bifurcation of E_0 are shown in Figs. 5 and 6. For $\tau_1 > 0$ and $\tau_2 = 2 \in (0, 3.8658)$, we get $\tilde{\omega}_1^0 = 1.2902$ and $\tilde{\tau}_1^0 = 1.2340$. The corresponding asymptotic stability and the Hopf bifurcation of E_0 are plotted in Figs. 7 and 8.

For the second set of parameter values (i.e., the third row in Table 1), we obtain $R_0 = 1.1746 (> 1)$. In this case, system (1) has a unique endemic equilibrium point $E_1 = (8.5135, 0.0787, 0.0708, 0.7236)$. For $\tau_1 = \tau_2 = 0$, we have $a_0^2 = 1$, $a_1^2 = 1.16365$, $a_2^2 = 0.4634$ and $a_3^2 = 0.0047$. Obviously, $a_1^2 a_2^2 > a_0^2 a_3^2$ and E_1 is asymptotically stable from Theorem 6 (Fig. 9). For $\tau_1 = 0$, $\tau_2 > 0$, we get $\bar{\omega}_2^0 = 0.2881$ and $\bar{\tau}_2^0 = 4.1563$. Using Theorem 7, we con-

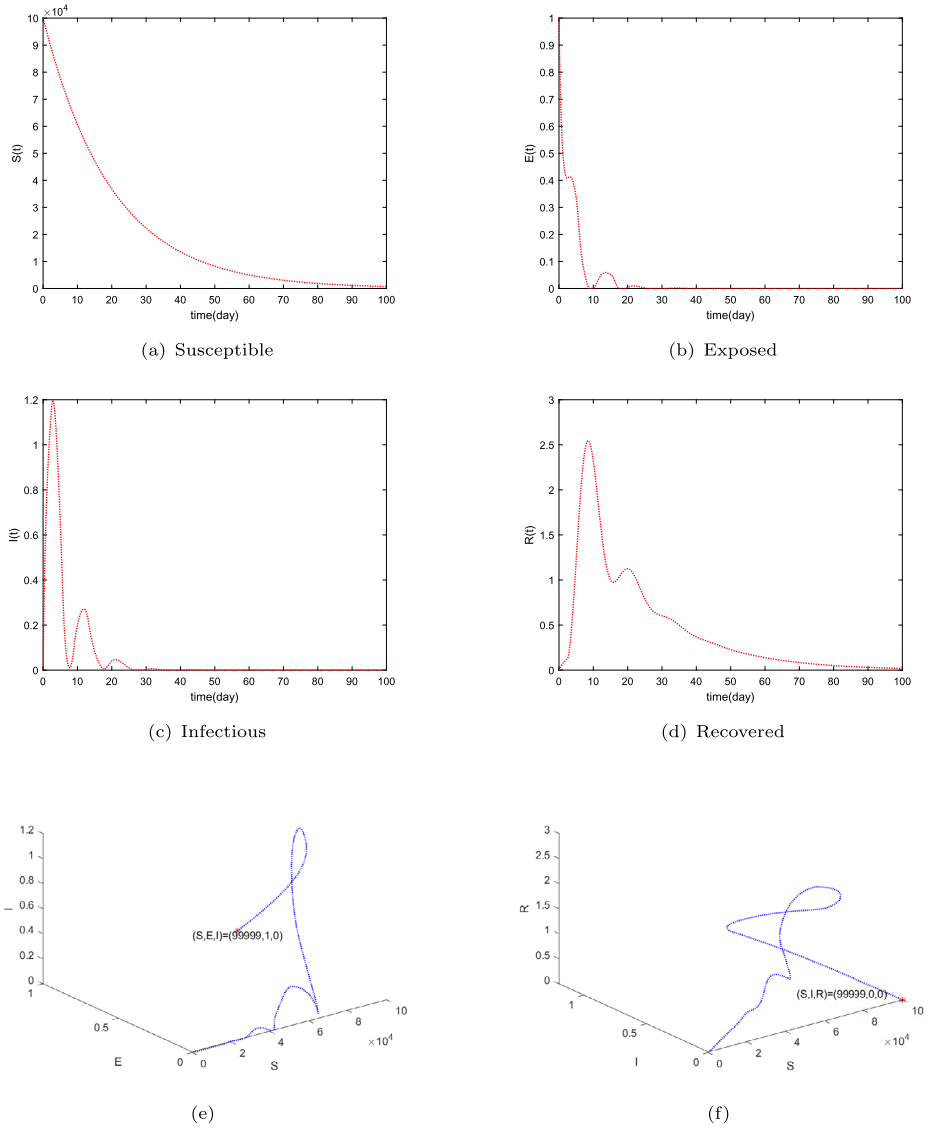

Figure 3 When $\tau_1 = 0$, E_0 is asymptotically stable for $\tau_2 = 2.5 < \tau_2^0 = 3.8658$

clude that E_1 is asymptotically stable when $\tau_2 \in (0, 4.1563)$ and that the Hopf bifurcation occurs when $\tau_2 = 4.1563$ (Figs. 10 and 11). For $\tau_1 > 0$ and $\tau_2 = 0$, we obtain $\bar{\omega}_1^0 = 1.0086$ and $\bar{\tau}_1^0 = 1.2326$. The corresponding asymptotic stability and the Hopf bifurcation are plotted in Figs. 12 and 13. For $\tau_1 > 0$ and $\tau_2 = 3.5 \in (0, 4.1563)$, we obtain $\hat{\omega}_1^0 = 1.8961$ and $\hat{\tau}_1^0 = 0.5437$. The corresponding asymptotic stability and the Hopf bifurcation are shown in Figs. 14 and 15.

5.2 Numerical results of optimal control problem

In this section, we will present numerical results for solving Problem (DOCP). Here, the delayed SEIR system (49) was solved using software package DDE23 in Matlab with delay arguments $\tau_1 = 0.5$ and $\tau_2 = 0.7$ and the initial condition $\varphi(t) = (99999, 1, 0, 0)^\top$ [14]. The weight coefficients in the cost functional (50) are chosen as $q_1 = 10^{-8}$, $q_2 = q_3 = 10^{-4}$, $r_1 =$

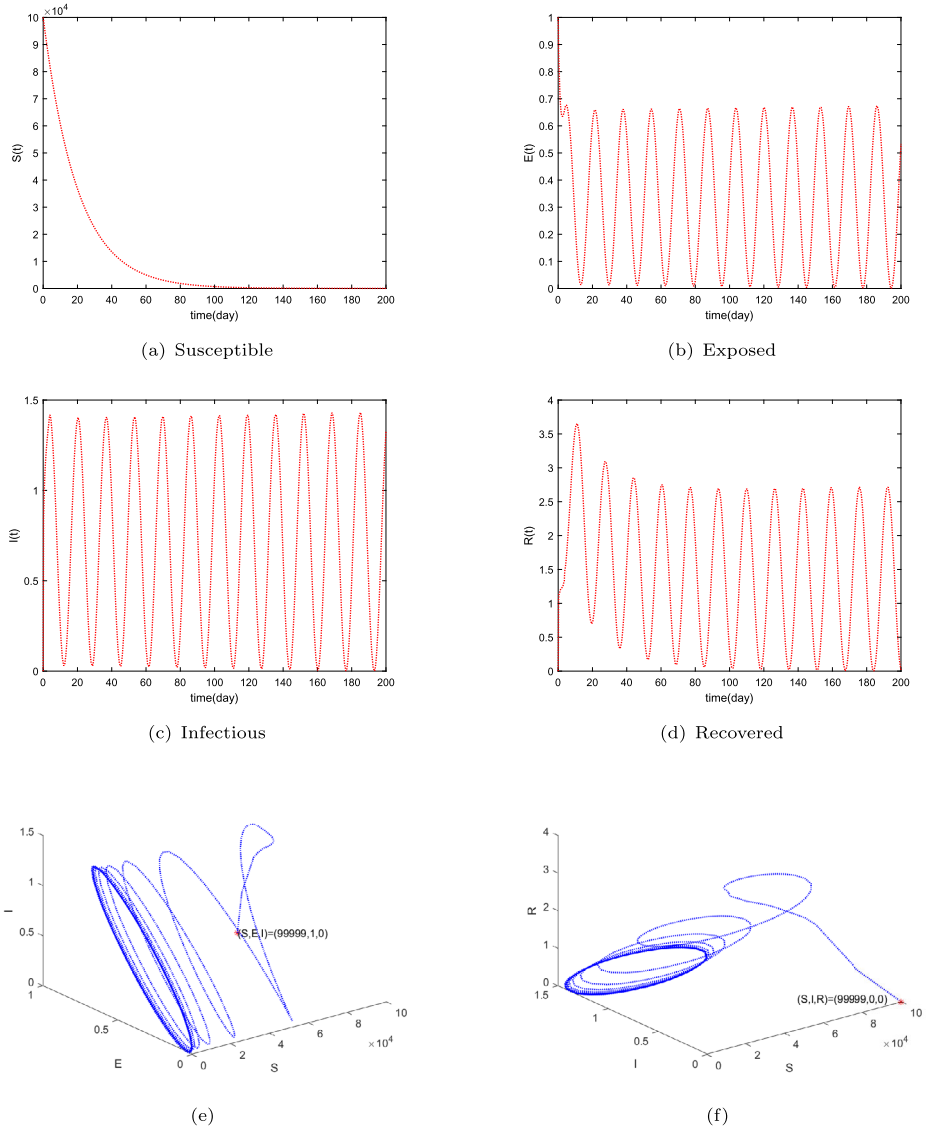

Figure 4 When $\tau_1 = 0$, E_0 is unstable for $\tau_2 = 3.87 > \tau_2^0 = 3.8658$

50 and $r_2 = 1$ [14]. In addition, we choose two sets of parameter values listed in Table 1 for calculating the optimal control strategies. As for the control boundaries, we assume that $u_1^{\max} = 0.07$ and $u_2^{\max} = 0.1$. Note that Problem (DOCP) was solved using forward-backward sweep method [35] in conjunction with the necessary optimality conditions in Theorem 10.

To explore the effects of each control means, we set up the following control scheme.

(i) Strategy A: Social contact only (u_1).

(ii) Strategy B: Pharmaceutical intervention only (u_2).

(iii) Strategy C: Social contact + Pharmaceutical intervention (u_1, u_2).

For the first set of parameters (i.e., the second row in Table 1), we solve Problem (DOCP) and obtain the optimal control strategies u_1^* and u_2^* shown in Fig. 16. The state trajectories corresponding to different control strategies, i.e., $u_1 = u_2 = 0$, $u_1 = u_1^*$ and $u_2 = 0$, $u_1 = 0$

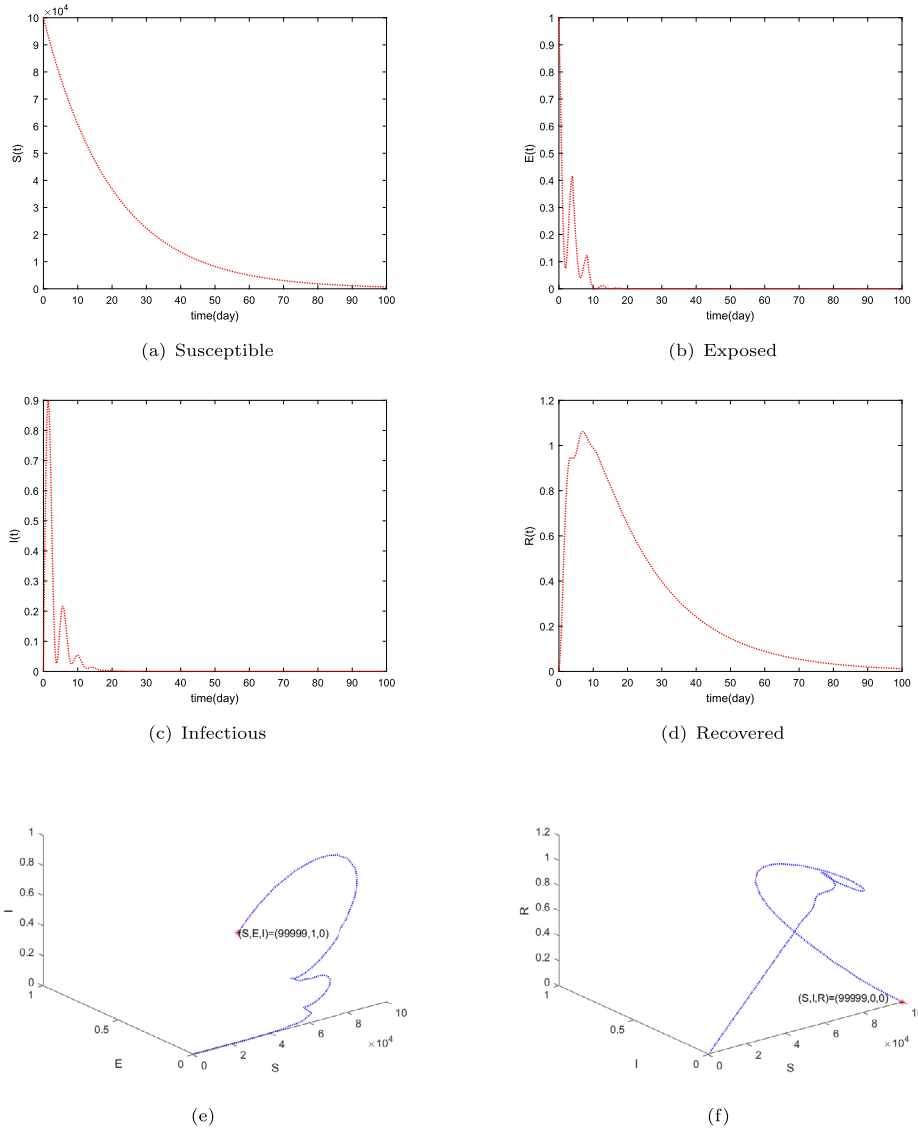

Figure 5 When $\tau_2 = 0$, E_0 is asymptotically stable for $\tau_1 = 0.9 < \tau_1^0 = 1.4683$

and $u_2 = u_2^*$, and $u_1 = u_1^*$ and $u_2 = u_2^*$, are plotted in Fig. 17. Similarly, for the second set of parameters (i.e., the third row in Table 1), we also solve Problem (DOCP) and obtain the optimal control strategies $\bar{u}_1^*$ and $\bar{u}_2^*$ depicted in Fig. 18. The state trajectories corresponding to different control strategies, i.e., $u_1 = u_2 = 0$, $u_1 = \bar{u}_1^*$ and $u_2 = 0$, $u_1 = 0$ and $u_2 = \bar{u}_2^*$, and $u_1 = \bar{u}_1^*$ and $u_2 = \bar{u}_2^*$, are plotted in Fig. 19.

From Figs. 16 and 18, we can see that, for the social contact u_1, it begins with the maximal value of 0.07, keeps the maximal value for a period of time, and then decreases to zero. This is mainly because, in the case of a sudden outbreak of COVID-19, quarantine measures are effective in stopping the spread of the disease by cutting off the route of transmission in the real world. As for the pharmacological intervention u_2, since the pharmacological intervention for the infected individuals is not immediately administered, it starts from

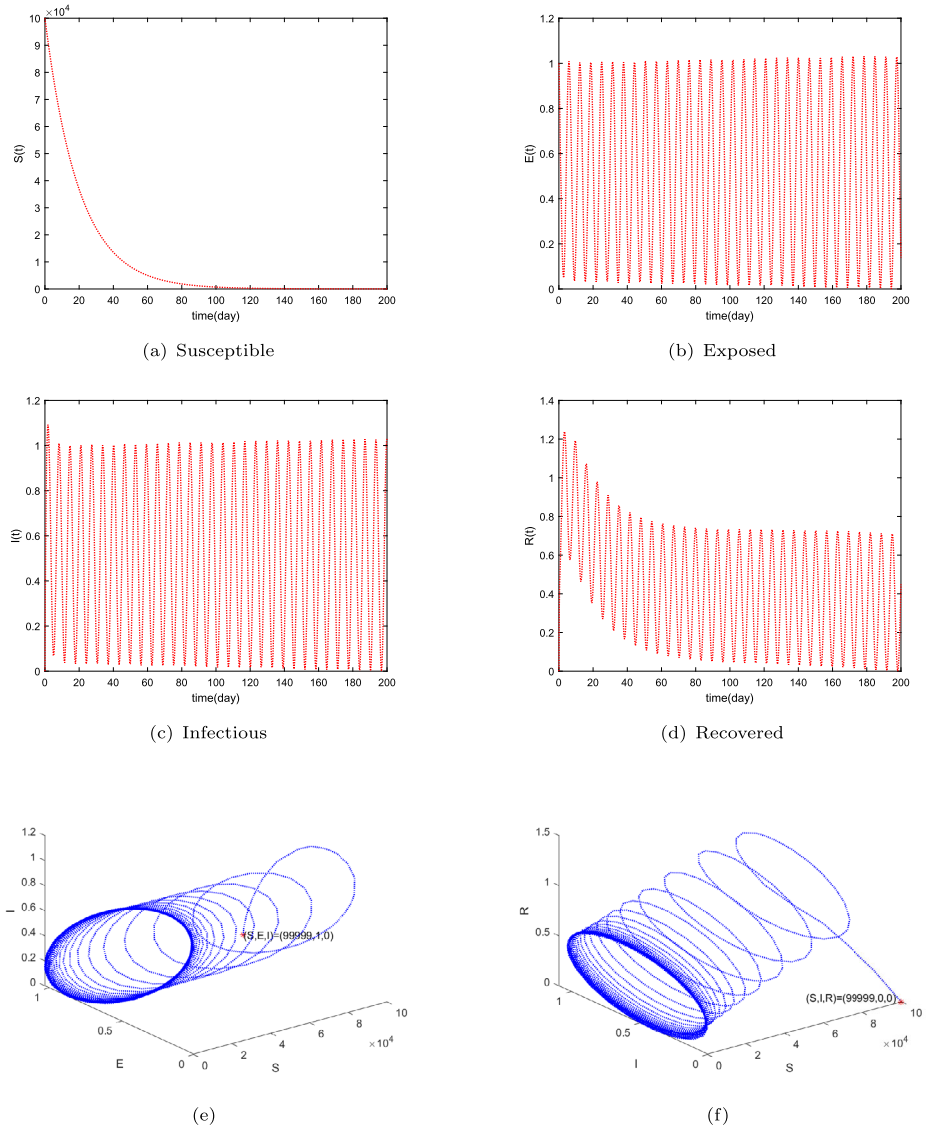

Figure 6 When $\tau_2 = 0$, E_0 is unstable for $\tau_1 = 1.4684 > \tau_1^0 = 1.4683$

the minimal value of zero, rapidly increases to the maximal value of 0.1, maintains at this maximal value for a period of time, and ultimately reduces to zero.

From Figs. 17(b), 17(c), 19(b), and 19(c), it can be seen that the number of exposed and infected individuals under no control is the highest, while the lowest number of exposed and infected individuals is under strategy C. Moreover, the implementation of u_1 can decrease the number of both exposed and infectious individuals, while the implementation of u_2 is particularly effective in reducing the number of infected individuals. Nevertheless, relying solely on one control measure (strategies A and B) or not implementing any control measures at all is less effective than the optimal control strategy C.

For strategy C, we also solved the optimal control problem without delay. The computed optimal control strategies under two sets of parameter values are also illustrated in Figs. 16 and 18, respectively. Under the optimal control strategies in Figs. 16 and 18,

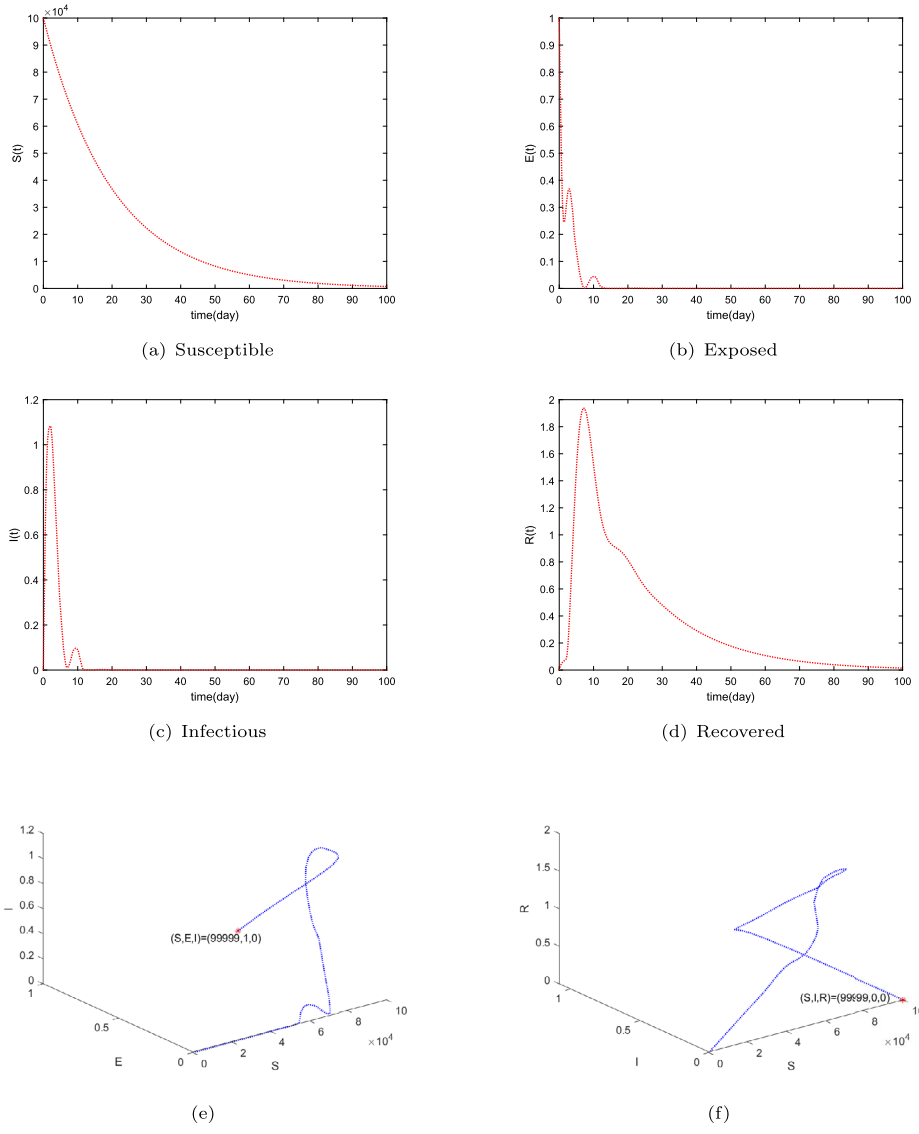

Figure 7 When $\tau_2 = 2$, E_0 is asymptotically stable for $\tau_1 = 0.5 < \tilde{\tau}_1^0 = 1.2340$

the corresponding optimal state trajectories are depicted in Figs. 20 and 21. From Figs. 20 and 21, we observe that the peaks of infected individuals for the cases with $\tau_1 = 0.5$ and $\tau_2 = 0.7$ are higher than those without delay. This implies that time delays could aggravate the transmission of COVID-19. As a result, to minimize the number of infections, effective control strategies should be implemented as soon as possible.

6 Conclusion

In this paper, we have studied the dynamics analysis and optimal control of the delayed SEIR model in the COVID-19 epidemic. Two delays representing the incubation and recovery periods in COVID-19 virus transmission have been introduced. A key issue with delays describing the incubation and recovery periods is whether they cause sustained oscillations. This was investigated through Hopf bifurcation analysis. By using the charac-

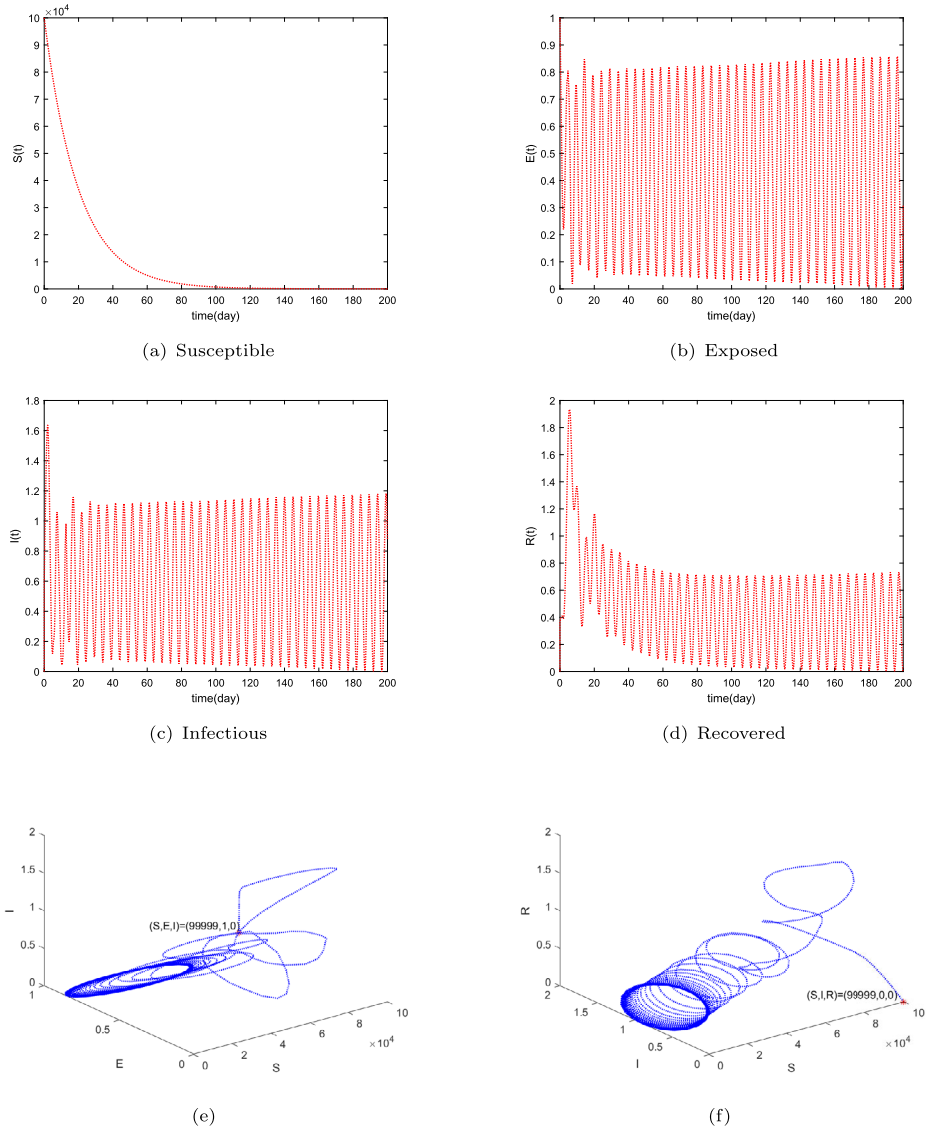

Figure 8 When $\tau_2 = 2$, E_0 is unstable for $\tau_1 = 1.235 > \tau_1^0 = 1.2340$

teristic equations of delay differential equations, the existence of Hopf bifurcations at the disease-free and endemic equilibrium points was established. It has been shown that under some conditions, delays representing the incubation and recovery periods may destabilize the disease-free and endemic equilibrium points and cause the population to fluctuate. From Theorems 3, 4, 5, 7, 8, and 9, we see that thresholds for two delays were identified to characterize the existence of Hopf bifurcations at the disease-free and endemic equilibrium points. In addition, two controls representing the social contact and pharmaceutical intervention have also been introduced. The delay optimal control problem was formulated, and its necessary optimality conditions were exploited to solve the optimal controls. Numerical simulation results indicate that the pharmacological intervention was more effective for hospitalized patients, whereas suppression of social contact reduced the num-

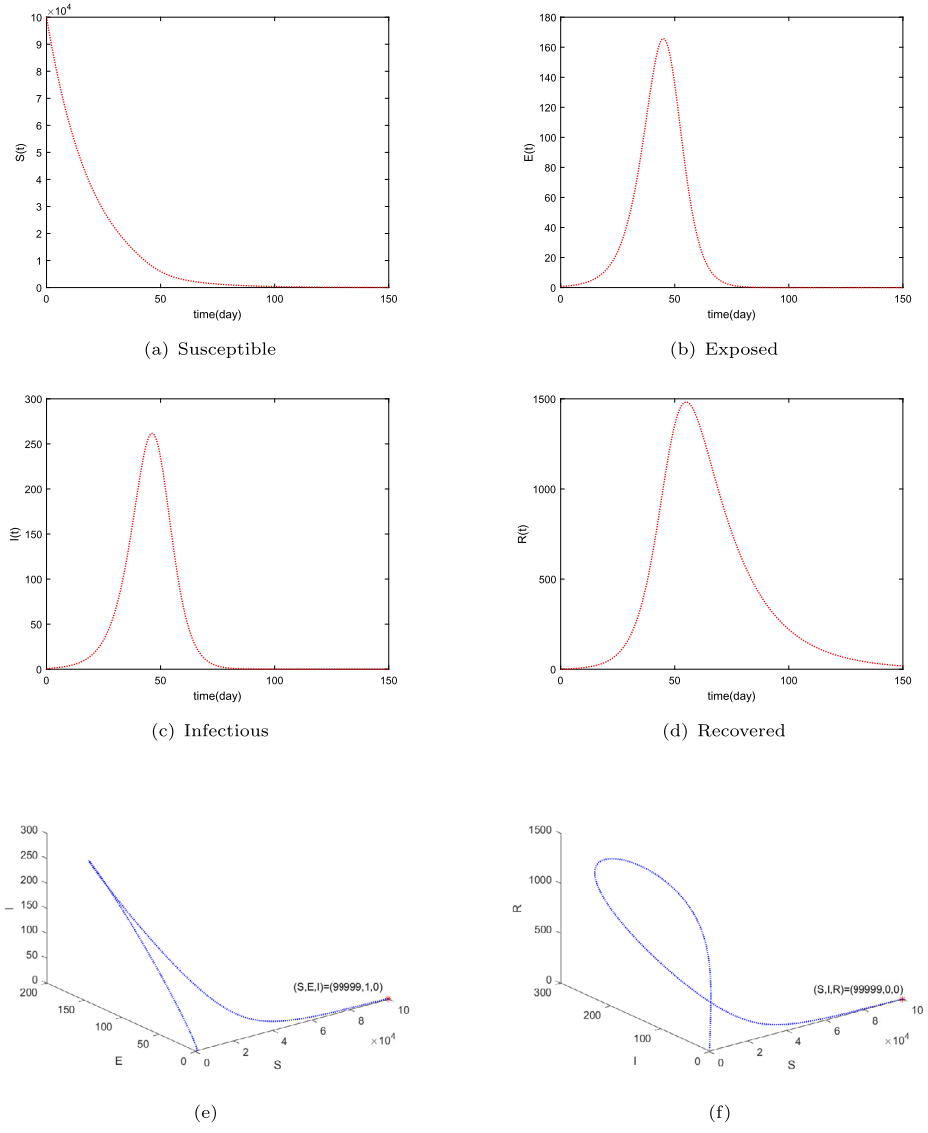

Figure 9 When $\tau_1 = \tau_2 = 0$, E_1 is asymptotically stable

ber of exposed individuals. More importantly, the obtained optimal strategies are effective in preventing and controlling the spread of COVID-19 infection.

We note that the effect of vaccination is ignored in systems (1) and (47). Vaccination has played a major role in preventing the spread of COVID-19 [36–38]. Moreover, the fractional derivative can be regarded as the generalization of the traditional integer derivative, which shows many important properties that the integer derivative does not have [39–44]. Many scholars have applied fractional derivative differential equations to study the spread of COVID-19 [45–47]. As a result, it is worthwhile to investigate the fractional optimal control of the COVID-19 epidemic by incorporating vaccination. This will be left for future research work.

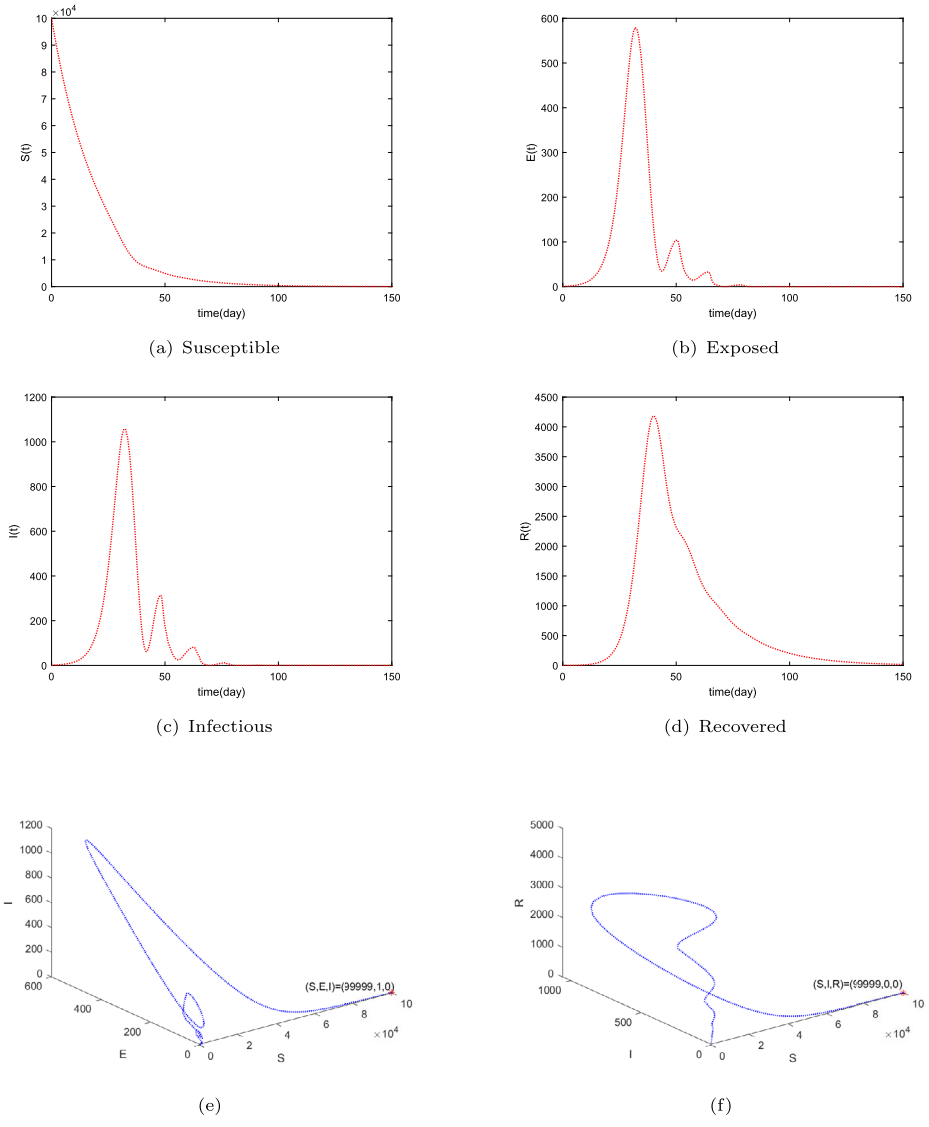

(a) Susceptible (b) Exposed (c) Infectious (d) Recovered (e) (f)

Figure 10 When $\tau_1 = 0$, E_1 is asymptotically stable for $\tau_2 = 3.1 < \tilde{\tau}_2^0 = 4.1563$

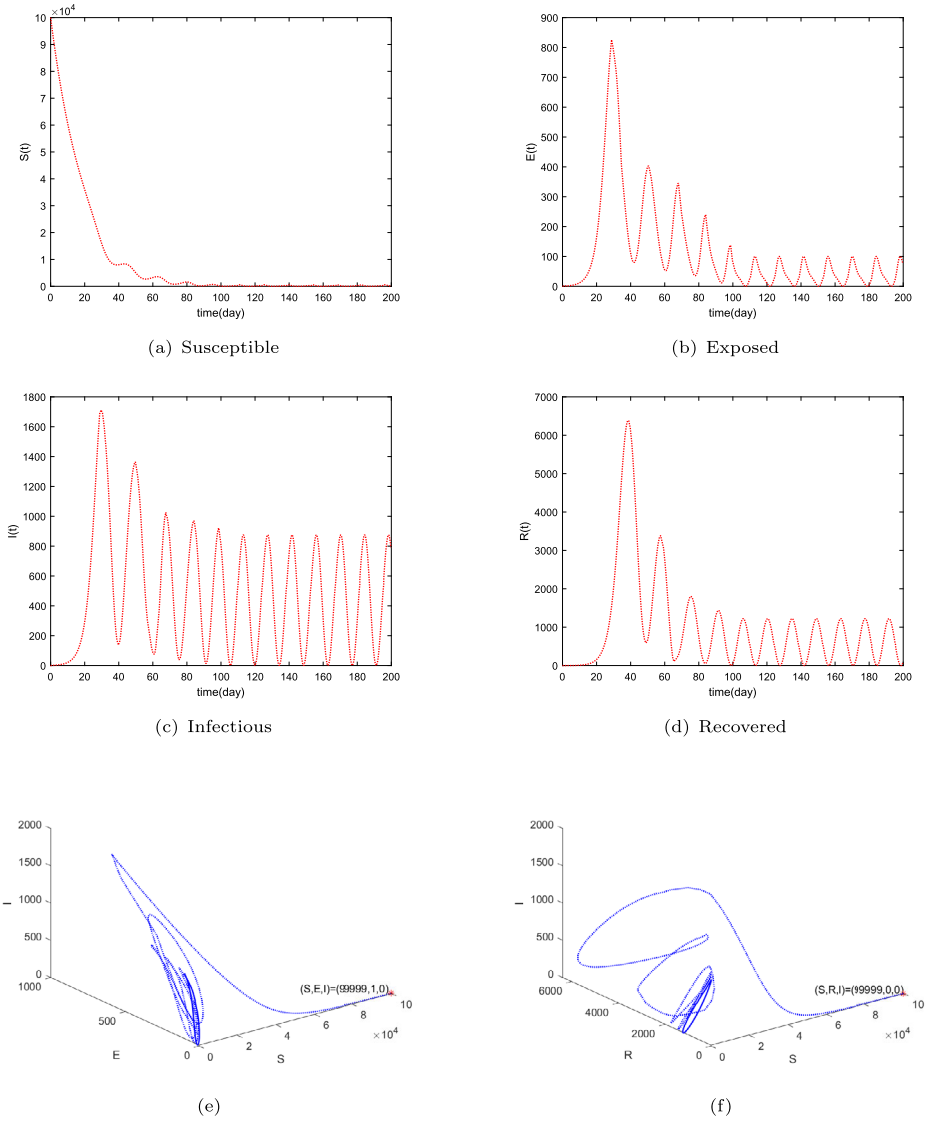

(a) Susceptible (b) Exposed

(c) Infectious (d) Recovered

(e) (f)

Figure 11 When $\tau_1 = 0$, E_1 is unstable for $\tau_2 = 4.16 > \tilde{\tau}_2^0 = 4.1563$

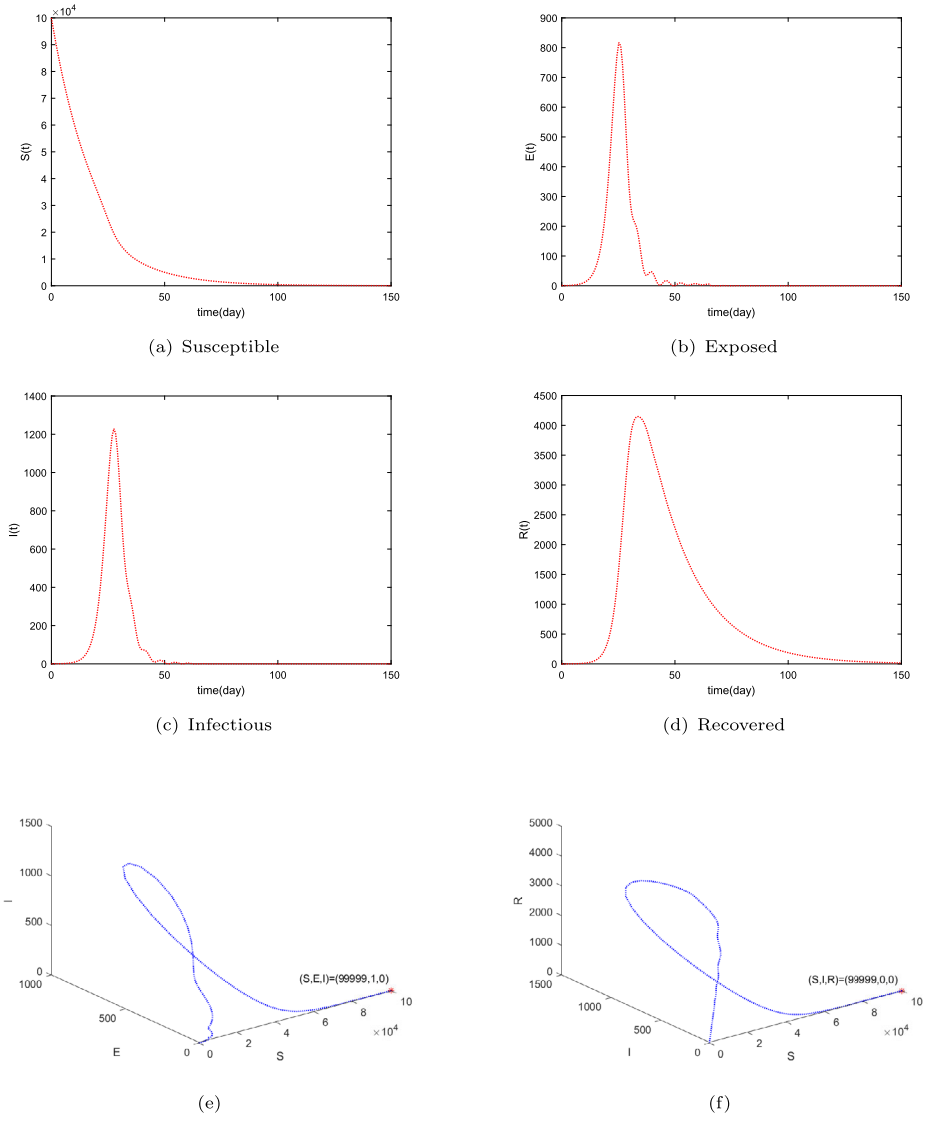

(a) Susceptible (b) Exposed (c) Infectious (d) Recovered (e) (f)

Figure 12 When $\tau_2 = 0$, E_1 is asymptotically stable for $\tau_1 = 1.1 < \tilde{\tau}_1^0 = 1.2326$

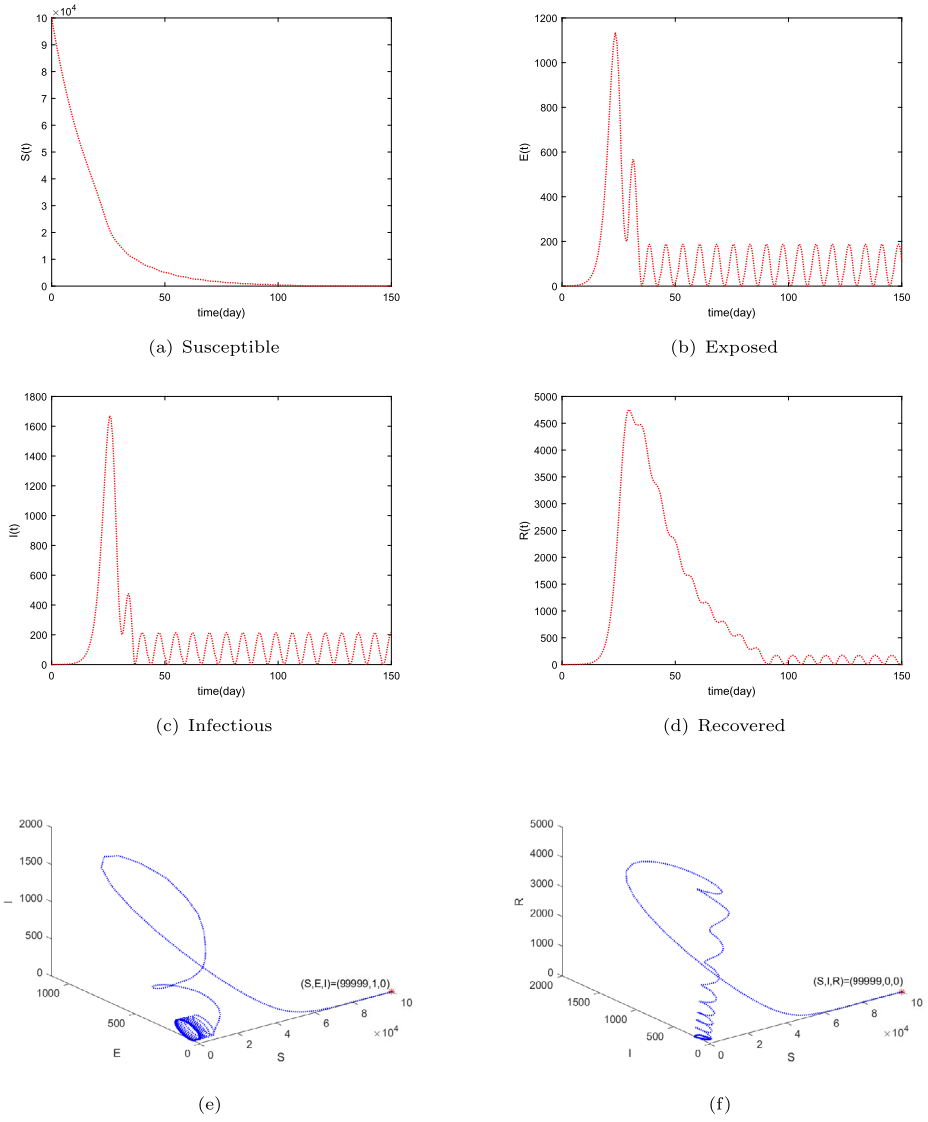

(a) Susceptible (b) Exposed

(c) Infectious (d) Recovered

(e) (f)

Figure 13 When $\tau_2 = 0$, E_1 is unstable for $\tau_1 = 1.24 > \tilde{\tau}_1^0 = 1.2326$

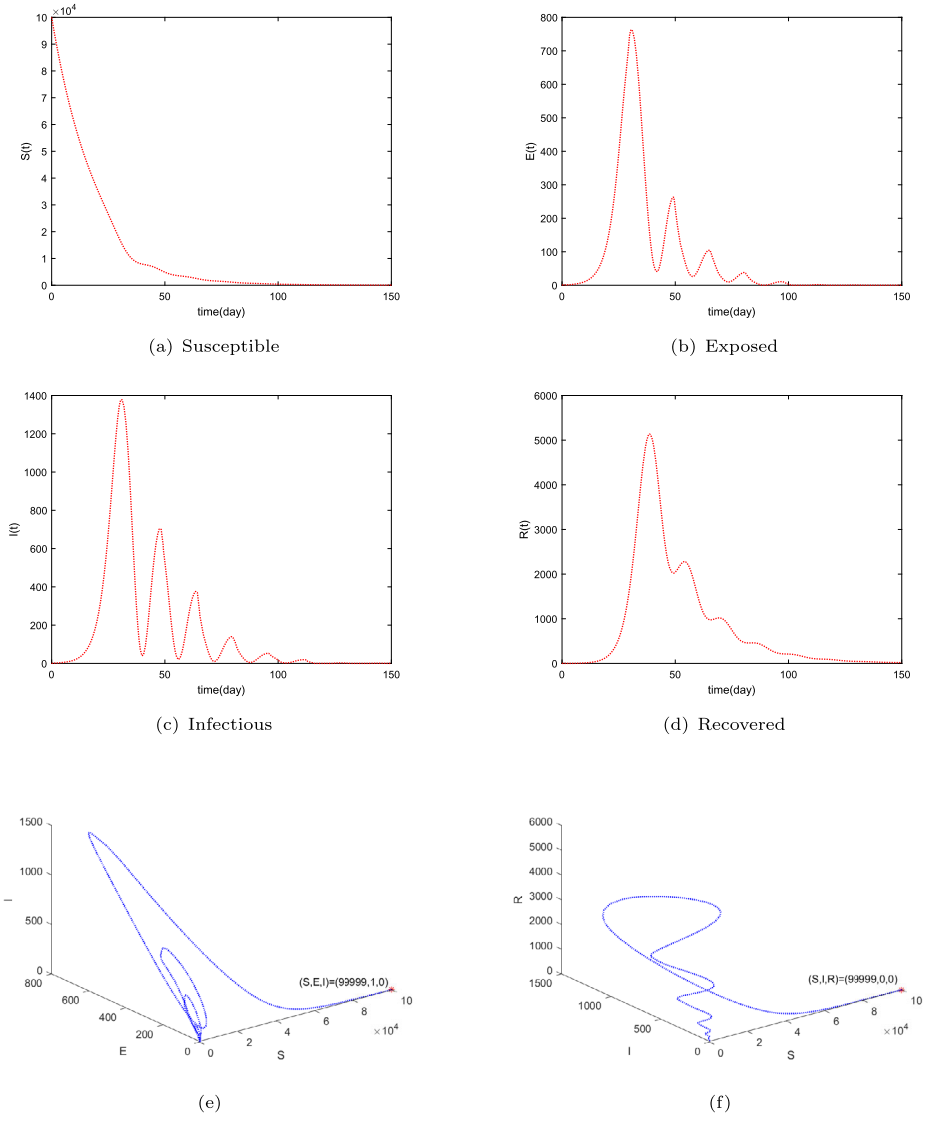

(a) Susceptible (b) Exposed

(c) Infectious (d) Recovered

(e) (f)

Figure 14 When $\tau_2 = 3.5$, E_1 is asymptotically stable for $\tau_1 = 0.05 < \hat{\tau}_1^0 = 0.5437$

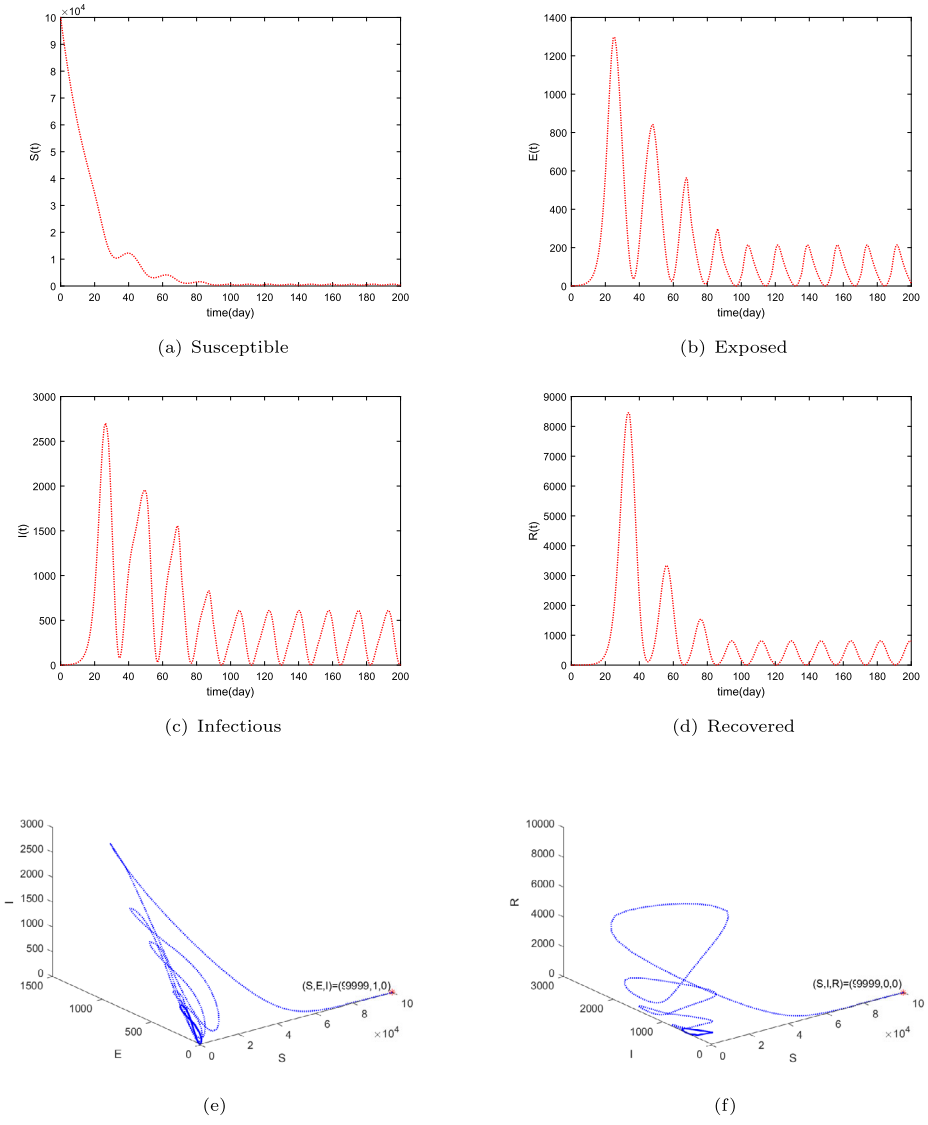

Figure 15 When $\tau_2 = 3.5$, E_1 is unstable for $\tau_1 = 0.55 > \hat{\tau}_1^0 = 0.5437$

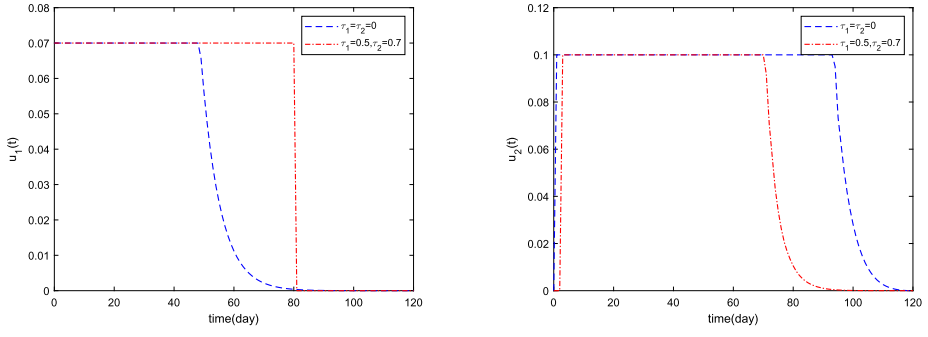

Figure 16 The optimal control strategies under the first set of parameter values

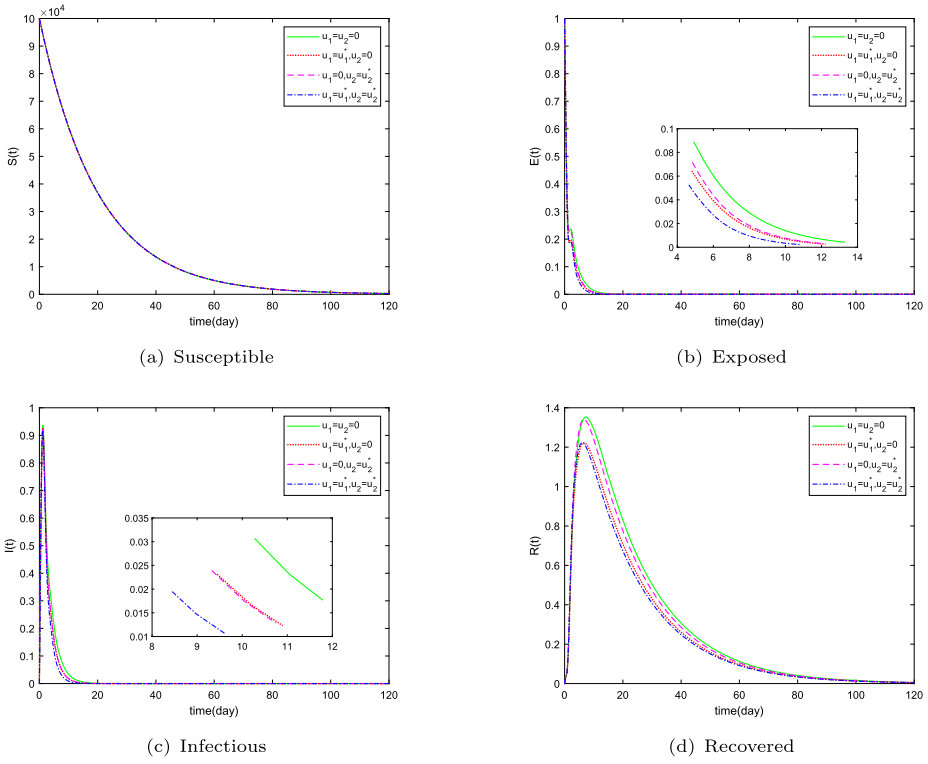

(a) Susceptible (b) Exposed

(c) Infectious (d) Recovered

Figure 17 State trajectories with different control strategies under the first set of parameter values

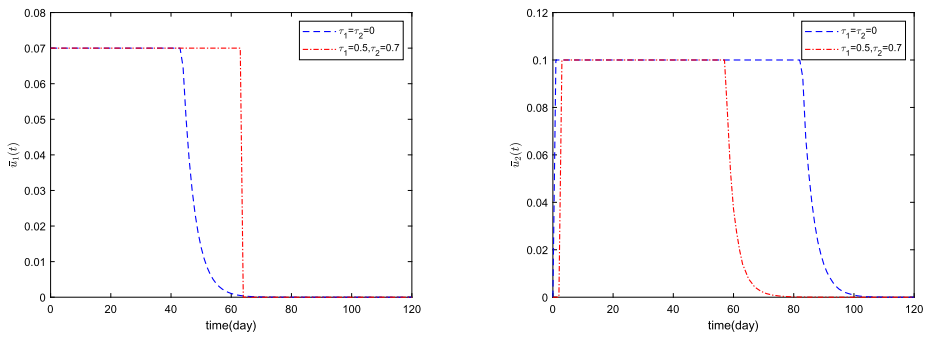

Figure 18 The optimal control strategies under the second set of parameter values

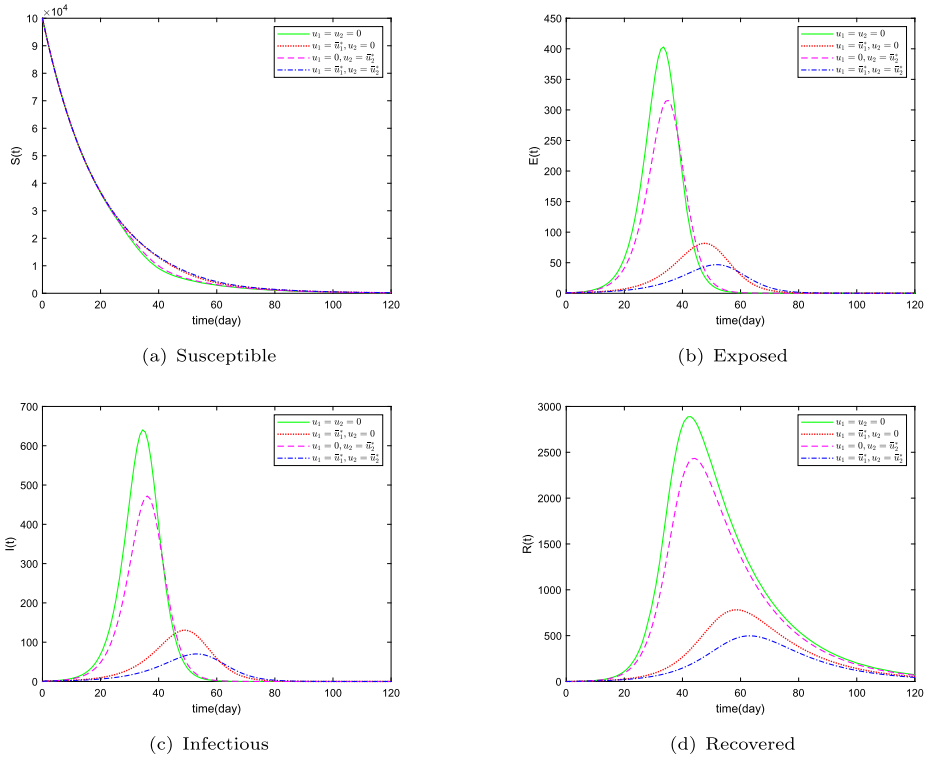

(a) Susceptible (b) Exposed

(c) Infectious (d) Recovered

Figure 19 State trajectories with different control strategies under the second set of parameter values

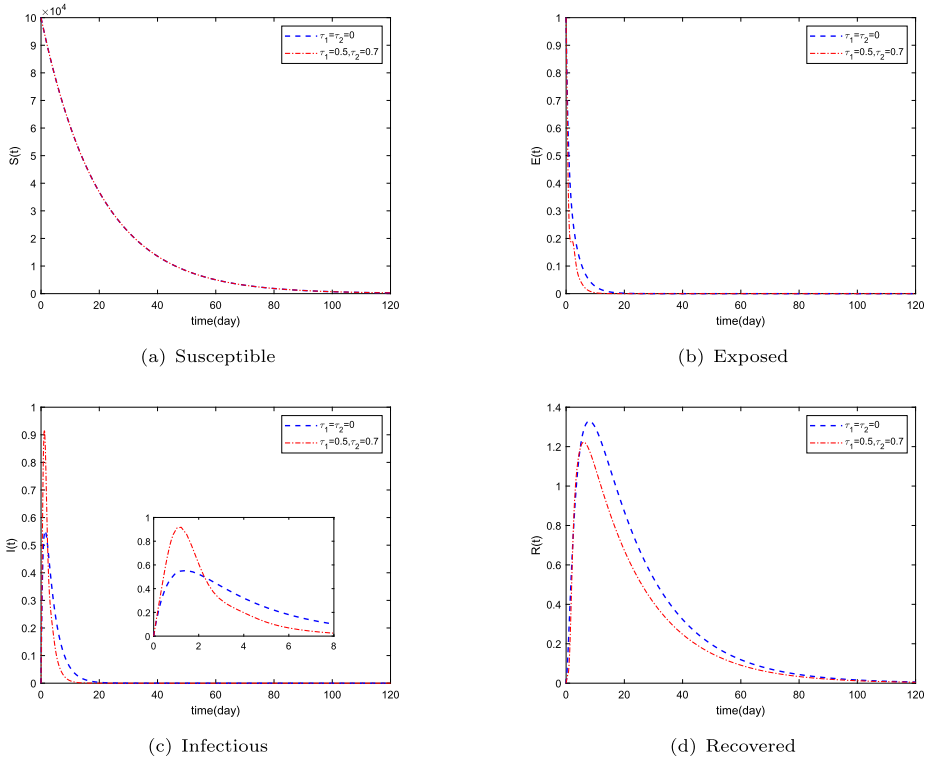

(a) Susceptible (b) Exposed

(c) Infectious (d) Recovered

Figure 20 Optimal state trajectories under the first set of parameter values

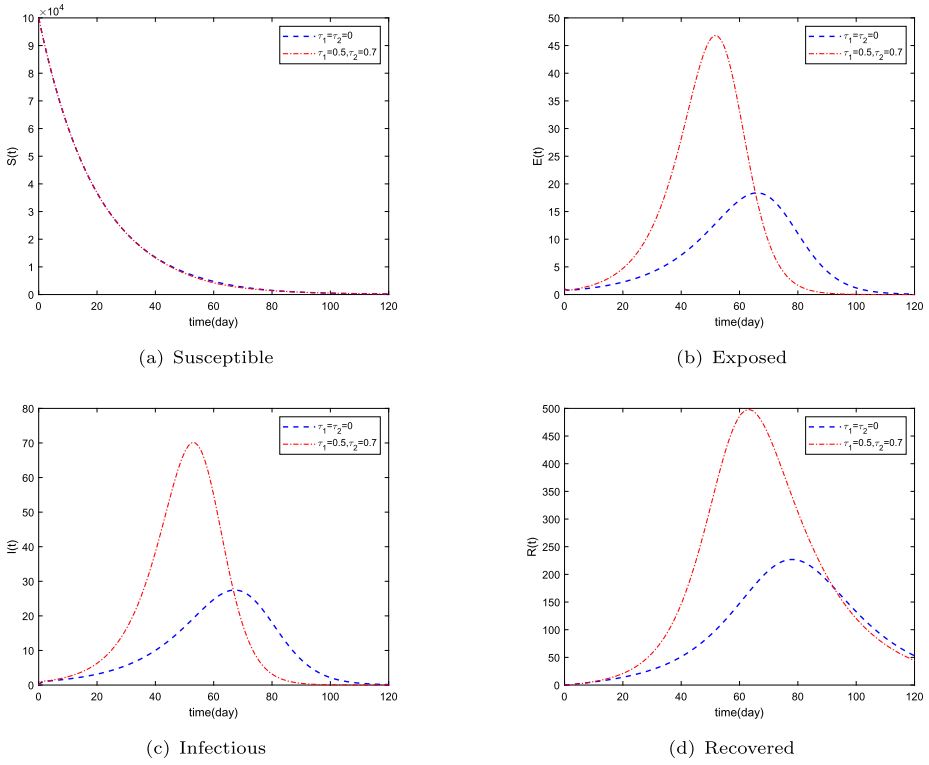

(a) Susceptible (b) Exposed

(c) Infectious (d) Recovered

Figure 21 Optimal state trajectories under the second set of parameter values

Acknowledgements
The supports of National Natural Science Foundation of China (No. 12271307) and Shandong Province Natural Science Foundation of China (No. ZR2023MA054) are gratefully acknowledged.

Author contributions
C.L. and J.G. wrote the main manuscript and C.L. and J.K. revised the manuscript. All authors reviewed the manuscript

Data Availability
No datasets were generated or analysed during the current study.

Declarations

Competing interests
The authors declare no competing interests.

Author details
[1]School of Mathematics and Information Science, Shandong Technology and Business University, Yantai 264005, P.R. China. [2]Yantai Key Laboratory of Big Data Modeling and Intelligent Computing, Yantai, 264005, P.R. China. [3]School of Information and Electronic Engineering, Shandong Technology and Business University, Yantai 264005, P.R. China. [4]Department of Electrical Engineering, Faculty of Engineering, University Malaya, Kuala Lumpur 50603, Malaysia.

Received: 23 February 2024 Accepted: 19 April 2024 Published online: 09 May 2024

References

1. Kow, C.S., Hasan, S.S.: Do sleep quality and sleep duration before or after COVID-19 vaccination affect antibody response? Chronobiol. Int. **38**, 941–943 (2021)
2. Avadhani, A., Cardinale, M., Akintade, B.: COVID-19 pneumonia: what APRNs should know. Nurse Pract. **46**, 22–28 (2021)
3. Coronavirus Cases. https://www.worldometers.info/coronavirus/
4. Kermack, W.O., McKendrick, A.G.: A contribution to the mathematical theory of epidemics. Proc. R. Soc. Lond. **115**, 700–721 (1927)
5. Krämer, A., Kretzchmar, M., Kricheberg, K.: Modern Infectious Disease Epidemiology. Springer, New York (2010)
6. Li, M.Y.: An Introduction to Mathematical Modeling of Infectious Diseases. Springer, Cham (2018)

7. Julien, A., Portet, S.: A simple model for COVID-19. Infect. Dis. Model. **5**, 309–315 (2020)
8. Awasthi, A.: A mathematical model for transmission dynamics of COVID-19 infection. Eur. Phys. J. Plus **138**, 285 (2023)
9. Xu, C., Yu, Y., Ren, G., Sun, Y., Si, X.: Stability analysis and optimal control of a fractional-order generalized SEIR model for the COVID-19 pandemic. Appl. Math. Comput. **457**, 128210 (2023)
10. Nesteruk, I.: Simulations and predictions of COVID-19 pandemic with the use of SIR model. Innov. Biosyst. Bioeng. **4**, 110–121 (2020)
11. Cooper, I., Mondal, A., Antonopoulos, C.G.: A SIR model assumption for the spread of COVID-19 in different communities. Chaos Solitons Fractals **139**, 110057 (2020)
12. Annas, S., Pratama, M.I., Rifandi, M., Sanusi, W., Side, S.: Stability analysis and numerical simulation of SEIR model for pandemic COVID-19 spread in Indonesia. Chaos Solitons Fractals **139**, 110072 (2020)
13. Ahmed, N., Elsonbaty, A., Raza, A., Rfiq, M., Adel, W.: Numerical simulation and stability analysis of a novel reaction-diffusion COVID-19 model. Nonlinear Dyn. **106**, 1293–1310 (2021)
14. Biswas, S.K., Ahmed, N.U.: Mathematical modeling and optimal intervention of COVID-19 outbreak. Quant. Biol. **1**, 84–92 (2021)
15. Kouidere, A., EL Youssoufi, L., Ferjouchia, H., Balatif, O., Rachik, M.: Optimal control of mathematical modeling of the spread of the COVID pandemic with highlighting the negative impact of quarantine on diabetics people with cost-effectiveness. Chaos Solitons Fractals **145**, 110777 (2021)
16. Deressa, C.T., Duressa, G.F.: Modeling and optimal control analysis of transmission dynamics of COVID-19: the case of Ethiopia. Alex. Eng. J. **60**, 719–732 (2021)
17. Ahmed, M., Masud, M., Sarker, M.: Bifurcation analysis and optimal control of discrete SIR model for COVID-19. Chaos Solitons Fractals **174**, 113899 (2023)
18. Guo, Y., Li, T.: Modelling the competitive transmission of the Omecron strain and Delta strain of COVID-19. J. Math. Anal. Appl. **526**, 127283 (2023)
19. Chen, Y., Cheng, J., Jiang, Y., Liu, K.: A time delay dynamic system with external source for the local outbreak of 2019-nCoV. Appl. Anal. **101**, 146–157 (2022)
20. Paul, S., Lorin, E.: Estimation of COVID-19 recovery and decease periods in Canada using delay model. Sci. Rep. **11**, 23763 (2021)
21. Liu, C., Loxton, R., Teo, K.L.: A computational method for solving time-delay optimal control problems with free terminal time. Syst. Control Lett. **72**, 53–60 (2014)
22. Liu, C., Loxton, R., Teo, K.L.: Optimal parameter selection for nonlinear multistage systems with time-delays. Comput. Optim. Appl. **59**, 285–306 (2014)
23. Liu, C., Loxton, R., Teo, K.L.: Switching time and parameter optimization in nonlinear switched systems with multiple time-delays. J. Optim. Theory Appl. **163**, 957–988 (2014)
24. Liu, C., Gong, Z., Teo, K.L., Sun, J., Caccetta, L.: Robust multi-objective optimal switching control arising in 1, 3-propanediol microbial fed-batch process. Nonlinear Anal. Hybrid Syst. **25**, 1–20 (2017)
25. Liu, C., Loxton, R., Lin, Q., Teo, K.L.: Dynamic optimization for switched time-delay systems with state-dependent switching conditions. SIAM J. Control Optim. **56**, 3499–3523 (2018)
26. Liu, C., Loxton, R., Teo, K.L., Wang, S.: Optimal state-delay control in nonlinear dynamic systems. Automatica **135**, 109981 (2022)
27. Smith, H.L.: An Introduction to the Theory of Competitive and Cooperative Systems. Am. Math. Soc., Rhode Island (1995)
28. Van den Driessche, P., Watmough, J.: Reproduction numbers and sub-threshold endemic equilibria for compartmental models of disease transmission. Math. Biosci. **180**, 29–48 (2002)
29. Cesari, L.: Asymptotic Behavior and Stability Problems in Ordinary Differential Equations. Springer, Berlin (2012)
30. Bianca, C., Ferrara, M., Guerrini, L.: The Cai model with time delay: existence of periodic solutions and asymptotic analysis. Appl. Math. Inf. Sci. **7**, 21–27 (2013)
31. Hassard, B.D., Kazarinoff, N.D., Wan, Y.H.: Theory and Applications of Hopf Bifurcation. Cambridge University Press, Cambridge (1981)
32. Li, H., Liu, X., Yan, R., Liu, C.: Hopf bifurcation analysis of a tumor virotherapy model with two time delays. Phys. A, Stat. Mech. Appl. **553**, 124266 (2020)
33. Ruan, S., Wei, J.: On the zeros of a third degree exponential polynomial with applications to a delayed model for the control of testosterone secretion. Math. Med. Biol. **18**, 41–52 (2001)
34. Ray, W.H., Soliman, M.A.: The optimal control of processes containing pure time delays – I necessary conditions for an optimum. Chem. Eng. Sci. **25**, 1911–1925 (1970)
35. Lenhart, S., Workman, J.T.: Optimal Control Applied to Biological Models. CRC Press, London (2007)
36. Libotte, G.B., Lobato, F.S., Platt, G.M., Neto, A.J.S.: Determination of an optimal control strategy for vaccine administration in COVID-19 pandemic treatment. Comput. Methods Programs Biomed. **196**, 105664 (2020)
37. Li, T., Guo, Y.: Modeling and optimal control of mutated COVID-19 (Delta strain) with imperfect vaccination. Chaos Solitons Fractals **156**, 111825 (2022)
38. ElHassan, A., AbuHour, Y., Ahmad, A.: An optimal control model for Covid-19 spread with impacts of vaccination and facemask. Heliyon **9**, e19848 (2023)
39. Liu, C.Y., Gong, Z., Yu, C., Wang, S., Teo, K.L.: Optimal control computation for nonlinear fractional time-delay systems with state inequality constraints. J. Optim. Theory Appl. **191**, 83–117 (2021)
40. Gong, Z., Liu, C., Teo, K.L., Wang, S., Wu, Y.H.: Numerical solution of free final time fractional optimal control problems. Appl. Math. Comput. **405**, 126270 (2021)
41. Liu, C., Gong, Z.H., Teo, K.L., Wang, S.: Optimal control of nonlinear fractional-order systems with multiple time-varying delays. J. Optim. Theory Appl. **193**, 856–876 (2022)
42. Liu, C., Gong, Z., Wang, S., Teo, K.L.: Numerical solution of delay fractional optimal control problems with free terminal time. Optim. Lett. **17**, 1359–1378 (2023)
43. Liu, C., Yu, C., Gong, Z., Cheong, H., Teo, K.L.: Numerical computation of optimal control problems with Atangana-Baleanu fractional derivatives. J. Optim. Theory Appl. **197**, 798–816 (2023)
44. Liu, C., Zhou, T., Gong, Z., Yi, X., Teo, K.L., Wang, S.: Robust optimal control of nonlinear fractional systems. Chaos Solitons Fractals **175**, 113964 (2023)

45. Panwar, V.S., Sheik Uduman, P.S., Gómez-Aguilar, J.F.: Mathematiacal modeling of coronavirus disease COVID-19 dynamics using CF, and ABC non-singular fractional derivatives. Chaos Solitons Fractals **145**, 110757 (2021)
46. Pandey, P., Chu, Y.M., Gómez-Aguilar, J.F., Jahanshahi, H., Aly, A.A.: A novel fractional mathematicatical model of COVID-19 epidemic considering quarantine and latent time. Results Phys. **26**, 104286 (2021)
47. Guo, Y., Li, T.: Fractional-order modeling and optimal control of a new online game addition model based on real data. Commun. Nonlinear Sci. Numer. **121**, 107221 (2023)

Publisher's Note